



# BRNO UNIVERSITY OF TECHNOLOGY

VYSOKÉ UČENÍ TECHNICKÉ V BRNĚ

## FACULTY OF ELECTRICAL ENGINEERING AND COMMUNICATION

FAKULTA ELEKTROTECHNIKY  
A KOMUNIKAČNÍCH TECHNOLOGIÍ

## DEPARTMENT OF RADIO ELECTRONICS

ÚSTAV RADIOELEKTRONIKY

## REFRACTIVE INDEX OF WATER MEDIUM FOR UWC

INDEX LOMU VODNÍHO PROSTŘEDÍ PRO UWC

### BACHELOR'S THESIS

BAKALÁŘSKÁ PRÁCE

### AUTHOR

AUTOR PRÁCE

Ondřej Foltyn

### SUPERVISOR

VEDOUCÍ PRÁCE

doc. Ing. Lucie Hudcová, Ph.D.

BRNO 2023

# Bakalářská práce

bakalářský studijní program **Elektronika a komunikační technologie**

Ústav radioelektroniky

**Student:** Ondřej Foltyn

**ID:** 230245

**Ročník:** 3

**Akademický rok:** 2022/23

**NÁZEV TÉMATU:**

## Index lomu vodního prostředí pro UWC

### POKYNY PRO VYPRACOVÁNÍ:

Seznamte se s optickými bezdrátovými spoji pracujícími ve vodním prostředí, tzv. Underwater Communications (UWC). Definujte výhody, nevýhody a vlastnosti těchto komunikačních systémů. Seznamte se se způsoby určování indexu lomu vodního prostředí pro celé spektrum optických vlnových délek. Na základě dostupných datasetů vytvořte světovou mapu s potřebnými vstupními parametry (např. salinita, teplota vody, hloubka dna) pro určení indexu lomu vodního prostředí pro různé hloubky. Mapa rozložení vstupních veličin vodního prostředí bude zohledňovat měsíce, případně roční období. Útlum vodního prostředí zanedbejte. Vytvořte program, který na základě vstupních parametrů vodního prostředí (vytvořené mapy) vypočte lokální hodnoty indexu lomu prostředí.

Vytvořte komplexní program, který umožní stanovit profil indexu lomu vodního prostředí mezi dvěma body na základě zvolených zeměpisných souřadnic a hloubky pod vodní hladinou. Pro trasu mezi těmito body vykreslete šíření optického svazku o vhodné vybrané vlnové délce.

### DOPORUČENÁ LITERATURA:

[1] Index of Refraction of Seawater and Freshwater as a Function of Wavelength and Temperature [online]. 2022 Oregon State University [cit. 23.05.2022]. Dostupné z: <http://research.engr.oregonstate.edu/parrish/index-refraction-seawater-and-freshwater-function-wavelength-and-temperature>

[2] Refractive index of H<sub>2</sub>O, D<sub>2</sub>O (Water, heavy water, ice) - Kedenburg. RefractiveIndex.INFO - Refractive index database [online]. 2008 [cit. 23.05.2022]. Dostupné z: <https://refractiveindex.info/?shelf=main&book=H2O&page=Kedenburg>

**Termín zadání:** 6.2.2023

**Termín odevzdání:** 29.5.2023

**Vedoucí práce:** doc. Ing. Lucie Hudcová, Ph.D.

**doc. Ing. Lucie Hudcová, Ph.D.**  
předseda rady studijního programu

### UPOZORNĚNÍ:

Autor bakalářské práce nesmí při vytváření bakalářské práce porušit autorská práva třetích osob, zejména nesmí zasahovat nedovoleným způsobem do cizích autorských práv osobnostních a musí si být plně vědom následků porušení ustanovení § 11 a následujících autorského zákona č. 121/2000 Sb., včetně možných trestněprávních důsledků vyplývajících z ustanovení části druhé, hlavy VI. díl 4 Trestního zákoníku č.40/2009 Sb.

## **Abstract**

This work provides a general overview of the properties and possibilities of underwater wireless communication and its configurations. It also contains information about the refractive index in general and in the aquatic medium, its determination for certain environments, and the effect on underwater wireless communication. Finally, there is an overview of the structure and function of the program that was created.

## **Keywords**

Underwater optical wireless communication, refractive index, underwater medium, optical bundle, Python

## **Abstrakt**

Tato práce poskytuje obecný přehled vlastností a možností podvodní bezdrátové komunikace a jejích konfigurací. Obsahuje také informace o indexu lomu obecně a ve vodním médiu, dále jeho stanovení pro určité prostředí a jeho vlivu na podvodní bezdrátovou komunikaci. Na závěr je uveden přehled struktury a funkce vytvořeného programu.

## **Klíčová slova**

Podvodní optická bezdrátová komunikace, index lomu, podvodní prostředí, optický svazek, Python

# Rozšířený abstrakt

Optická bezdrátová podvodní komunikace (UOWC) je v poslední době čím dál tím více využívána ať už z pohledu průzkumu oceánů a moří, sledování znečištění, komunikaci mezi více podmořskými zařízeními aj. Její výhodou je dosažení vysokých přenosových rychlostí s nižší spotřebou energie a s celkovou menší hmotností. Problémem těchto komunikačních systémů je, že jsou ovlivňovány proměnlivým podvodním prostředím a jeho základními vlastnostmi. Kvůli těmto podmínkám nejsou podvodní optické bezdrátové spoje tak prozkoumány, jako třeba pozemní nebo vesmírné spoje.

Cílem této práce bylo seznámení se se základními vlastnostmi těchto komunikačních systémů, definovat jaké nabízí výhody a také nevýhody. Popsat vlastnosti a způsoby určování indexu lomu a na základě dostupných datasetů vytvořit světovou mapu, která bude zohledněna podle měsíců, jež bude určovat na základě potřebných vstupních parametrů lokální hodnotu indexu lomu a následně vykreslí šíření optického svazku a změnu indexu lomu pro trasu mezi dvěma zvolenými body.

Nejdříve je řešena problematika podvodní bezdrátové komunikace. Poté jsou definovány možnosti přenosu informací pomocí akustických, rádiových a optických vln. Následně jsou uvedeny možnosti a vlastnosti konfigurací optických podvodních bezdrátových spojů a představeny základní vlastnosti podvodního prostředí, jeho rozdělení a vliv na návrh podvodních bezdrátových spojů a na bezdrátové šíření informací.

Tato práce také nabízí stručný matematický a obecný popis indexu lomu z fyzikálního hlediska a jeho vlivu na UOWC a také jeho odvození z Maxwellových obecných rovnic pro šíření elektromagnetických vln.

Výstupem této práce je program, který je schopen určit změnu lokálního indexu vybraného bodu ve vodním prostředí, zadaného zeměpisnými souřadnicemi, hloubkou pod vodní hladinou a salinitou. Výpočet změny lokálního indexu vodního prostředí se provádí pro různé vlnové délky a jeho výsledky jsou přehledně zobrazeny v dostupné tabulce a vyneseny do grafu, jež jsou součástí daného programu.

Dále je tento program schopen určit profil indexu lomu vodního prostředí na trase mezi dvěma body, které jsou zadány stejným způsobem jako pro výpočet lokální změny indexu lomu, tedy zeměpisnými souřadnicemi, hloubkou obou bodů a výběrem typu vodního prostředí, na výběr jsou dvě možnosti, slaná voda se salinitou 35‰ a sladká voda se salinitou 0‰. Výsledky jsou obdobně vyneseny do grafů, které jsou součástí programu.

Výstupem bylo ověřeno, že se index lomu vodního prostředí mění v závislosti na změně několika různých parametrů. S volenou hloubkou pod vodní hladinou se zároveň mění i teplota vody v daném místě, což následně ovlivňuje index lomu. Výrazný vliv na index lomu má také zvolená vlnová délka, kdy se zvyšující se vlnovou délkou klesá hodnota indexu lomu. Index lomu je ovlivňován v reálném prostředí i velkým množstvím náhodných jevů jako jsou např. podvodní proudy nebo turbulence, tyto jevy se ale v této práci zanedbávají a pracuje se s prostředím bez útlumu.

## **Bibliographic citation**

FOLTYN, Ondřej. *Refractive index of water medium for UWC*. Brno: Brno University of Technology, Faculty of electrical engineering and communications, Dept. of Telecommunications, 2023. 40 p. Semestral thesis. Advised by doc. Ing. Lucie Hudcová, Ph.D.

## Author's Declaration

**Author:** *Ondřej Foltyn*

**Author's ID:** *230245*

**Paper type:** *Bachelor's Thesis*

**Academic year:** *2022/23*

**Topic:** *Refractive index of water medium for UWC*

I declare that I have written this paper independently, under the guidance of the advisor and using exclusively the technical references and other sources of information cited in the project and listed in the comprehensive bibliography at the end of the project.

As the author, I furthermore declare that, with respect to the creation of this paper, I have not infringed any copyright or violated anyone's personal and/or ownership rights. In this context, I am fully aware of the consequences of breaking Regulation S 11 of the Copyright Act No. 121/2000 Coll. of the Czech Republic, as amended, and of any breach of rights related to intellectual property or introduced within amendments to relevant Acts such as the Intellectual Property Act or the Criminal Code, Act No. 40/2009 Coll., Section 2, Head VI, Part 4.

Brno, May 29, 2023

-----  
author's signature

## **Acknowledgement**

I would especially like to thank my supervisor, doc. Ing. Lucie Hudcová, PhD for her patience and comprehension, valuable advice, held consultations, and support in working on this thesis throughout the semester.

Brno, May 29, 2023

-----  
Author's signature

# Contents

<b>FIGURES</b> .....	<b>8</b>
<b>TABLES</b> .....	<b>9</b>
<b>INTRODUCTION</b> .....	<b>10</b>
<b>1. UNDERWATER WIRELESS LINKS</b> .....	<b>11</b>
1.1 OPTIONS, TYPES, ADVANTAGES, AND DISADVANTAGES.....	11
1.2 LINK CONFIGURATIONS .....	12
1.2.1 LOS links .....	13
1.2.2 NLOS links .....	13
1.2.3 Retro-reflector links .....	14
1.3 PHYSICAL PROPERTIES OF THE UNDERWATER MEDIUM.....	15
1.3.1 Factors affecting the UOWC.....	16
1.3.2 Changes in temperatures in the aquatic environment.....	17
<b>2. REFRACTIVE INDEX OF THE UNDERWATER MEDIUM</b> .....	<b>18</b>
2.1 GENERAL EXPRESSION OF REFRACTIVE INDEX.....	19
2.1.1 Calculation of the refractive index .....	20
<b>3. WORLD MAP MODELLING</b> .....	<b>22</b>
3.1 PROGRAM PARAMETERS .....	22
3.1.1 Input parameters.....	24
3.2 STRUCTURE AND FUNCTION OF THE PROGRAM .....	24
3.2.1 Local refractive index of the transmitter for different wavelengths .....	31
3.2.2 Changes in refractive index on the path between two points .....	34
3.2.3 Beam spread over land and its length .....	40
3.2.4 Program limitations.....	42
3.2.5 Earth relief map.....	43
3.2.6 Changes in temperature on the path between transmitter and receiver .....	44
3.2.7 Temperature Profile .....	45
3.3 INSTRUCTIONS FOR OPERATING THE PROGRAM .....	47
<b>4. CONCLUSION</b> .....	<b>53</b>
<b>LITERATURE</b> .....	<b>54</b>
<b>SYMBOLS AND ABBREVIATIONS</b> .....	<b>55</b>
<b>LIST OF APPENDICES</b> .....	<b>56</b>



# FIGURES

1.1	Point-to-point LOS link configuration (taken from [2]).....	13
1.2	NLOS configuration a) reflective (taken from[2]) and b) diffuse (taken from [1]).....	14
1.3	Retro-reflection configuration (taken from [1]) .....	15
1.4	Geometry of inherent optical property (taken from [2]).....	16
1.5	Change of temperature with depth (taken from [4]) .....	17
3.1	Flowchart diagram of program function.....	23
3.2	An example of how the main program looks .....	24
3.3	The main window of the program after the startup .....	25
3.4	The first part of the main panel .....	25
3.5	The second part of the main panel.....	26
3.6	Program after selecting the map (January).....	27
3.7	Detailed image of rendered maps for a) February, and b) August .....	28
3.8	a) Program after inserting the coordinates, b) detailed view of the map.....	29
3.9	a) An example of calculated temperatures, b) Parameters of the selected point .....	30
3.10	Buttons for calculating refractive indices.....	30
3.11	Dependence of the refractive index on wavelengths for a temperature of 28.01 °C, a) calculated values in the table, b) calculated values in the graph .....	31
3.12	Dependence of the refractive index on wavelengths for a temperature of 28.01 °C and 10.76 °C ...	32
3.13	Dependence of the refractive index on wavelengths for a temperature of 20.00 °C for different salinities.....	33
3.14	Dependence of the refractive index on wavelengths for a temperature of 20.00 °C and 3.5 °C for freshwater .....	34
3.15	Refractive index changes in the environment between two points.....	35
3.16	Parameters of the First and the Second point .....	35
3.17	Beam spreading deflection .....	36
3.18	Beam spreading deflection for different wavelength.....	37
3.19	Forward propagation as an example of non-reciprocity .....	38
3.20	Reverse propagation as an example of non-reciprocity.....	39
3.21	Spreading the beam across the land a) A map for the month of July, b) a graph of how the refractive index changes on the path .....	41
3.22	The result of beam propagation between two points separated by land .....	42
3.23	World Relief map.....	43
3.24	Temperature changes on path between transmitter and receiver .....	44
3.25	Refractive index changes on path between transmitter and receiver .....	45
3.26	Temperature profile for different surface temperatures .....	46
3.27	Area for month selection and map rendering .....	47
3.28	Field for entering coordinates and depth below the water surface.....	47
3.29	Selecting one point and the choice of type of water environment .....	48
3.30	Calculating the local index of refraction and deleting the table.....	49
3.31	Selecting two different points using different buttons on the left and selecting wavelengths and calculating the refractive index profile on the right .....	50
3.32	Additional buttons.....	51

# TABLES

1.1	Comparison between different underwater wireless technologies [1], [2] .....	12
2.1	Table of coefficient values for fresh and saltwater (taken from [8]) .....	21

# INTRODUCTION

Recently, there has been a great interest in exploring the oceans and seas, which is why optical wireless communication is becoming increasingly widespread. Optical wireless communication can provide high transmission speeds with low power consumption and less total weight. However, underwater optical wireless links are not as explored as terrestrial and space links due to the very demanding conditions of the underwater medium. Despite the variable characteristics of ocean and seawater, UOWC (Underwater Optical Wireless Communication) is of great interest in the marine industry and related activities, such as military, tactical surveillance, pollution monitoring, offshore exploration and oceanography research, and others. These topics are discussed in more detail in Articles [1], [2].

This work is focused on approaching the properties of underwater wireless communication and the underwater medium itself from a physical point of view. The main objective of this work was to create a program that, depending on the input parameters, calculates the refractive index of the aquatic environment, and its propagation in the underwater medium between two points and plots the propagation of the optical beam for a path between these points.

The first part is focused on underwater wireless links. Clarification of the options of underwater wireless information transmission, types, and characteristics of configurations of individual links. Subsequently, the basic properties of the aquatic medium are presented, which affect the refractive index and thus the choice of underwater links and their possibilities.

The second part of this work focuses on the index of refraction. Its properties, general and mathematical description from a physical point of view and its influence on UOWC.

The last part presents the program itself, which is the output of this work. Its functions and features are described here. Furthermore, examples of achieved results and graphs are presented and described here.

# 1. UNDERWATER WIRELESS LINKS

Nowadays, an increasing variety of options are available for information propagation in underwater wireless communication. The most crucial factor when choosing is certain characteristics of the water medium, as the environment is highly variable and fundamental characteristics vary from shallow water to deep oceans. It also requires a thorough understanding of the complex underwater environment. Several factors have a significant impact on UOWC, these are:

- Underwater light attenuation [1], [2]
  - Absorption and scattering,
  - Physical obstruction,
- Change in the width of the UOWC links [1]
  - Turbulence,
  - Scintillation,
- Beam spreading [1]
  - Misalignment,
  - Scattering,
- Multipath interference,
- Background noise [1]
  - Noise from the Sun or other stellar (point) objects,
  - Scattered light collected by the receiver,
  - Added noise from signal sources.

Some more important factors will be further discussed later.

In terms of transmission, underwater wireless communication uses three carriers: acoustic, radio frequency, and optical. Each one has its distinctive characteristics, pros, and cons, such as different transmission speeds, the size of the transferred data, or a different transmission frequency band [1],[2].

## 1.1 Options, types, advantages, and disadvantages

Present technologies use acoustic waves. However, their performance is limited by low bandwidth, high transmission losses, high latency, and Doppler spread. Acoustic links can be classified as very long, long, medium, short, and very short depending on the transmission distance. Acoustic communication currently available can support data rates of tens of kbps for long distances and up to hundreds of kbps for short distances [1].

For transferring the high data rate, a good option for using the UWC are electromagnetic waves (EM) in the range of radio frequency (RF). The disadvantage is that the RF waves are highly attenuated by seawater and the attenuation also increases with the frequency. For choosing the EM speed, it is necessary to pay attention to the

used frequency and mainly to the characteristic properties of the underwater medium, such as permeability, permittivity, and others [1].

Optical waves are most commonly used for broadband transmission, capable of transmitting up to units of Gbps over short distances. However, they are mostly affected by other propagation effects such as scattering, dispersion, or beam steering. Although there is a large attenuation, in the electromagnetic underwater spectrum an optical window can be found around blue-green wavelengths where relatively little attenuation occurs [1].

Table 1.1 Comparison between different underwater wireless technologies [1], [2]

UWC technology	Data rate	Range	Latency	Speed (m/s)	Other properties
Acoustic	~ kbps	Up to dozens of km	High	1500 m/s	Bulky, costly, harmful to some marine life
RF (ELF and LF range)	~ Mbps	Long distances (range 30 – 300 Hz)	Moderate	$\approx 2,255 \times 10^8$	Bulky, costly, most tolerant to turbulence, required high transmitter power
RF (MF range)		Up to 10 km (300 kHz – 30 MHz)			
RF (VHF and UHF range)		High rates of 2,4 GHz and 5 GHz at short ranges			
Optical	~ Gbps	10 – 100 meters	Low	$\approx 2,255 \times 10^8$	Suffers from absorption and scattering, low cost

## 1.2 Link configurations

Nowadays, the configurations of optical links used for the transmission of the light beam are divided into three categories:

- 1) LOS (line-of-sight) links,
- 2) NLOS (non-line-of-sight) links,
- 3) Retro-reflector links [1], [2].

### 1.2.1 LOS links

LOS point-to-point connection between transmitter and receiver is the simplest and the most used configuration in UOWC. The configuration principle can be seen in Figure 1.1.

Transmission of these systems is based on using light sources, such as lasers. The detection of the light beam by the receiver is in the direct line from the transmitter. Therefore, high accuracy of pointing between the two static sensors (transmitter and receiver) is important.

The limit of the performance of these systems is the requirement of a very precise direction between the transmitter and the receiver, as there is a high chance of affecting the light beam, either in a turbulent underwater environment or due to the influence of various obstacles in turbid harbors or by underwater life such as schools of fish, etc. Thus, they work best in clean oceans [1], [2].



Fig. 1.1 Point-to-point LOS link configuration (taken from [2])

### 1.2.2 NLOS links

This configuration was designed as LOS links cannot always be used in practical systems and therefore overcome some interference factors and alignment restrictions. NLOS links have reduced routing and tracking requirements, especially in turbid environments, for clear water environments laser beam divergence needs to be increased mostly with LEDs or lasers. Furthermore, NLOS links can be reflective or diffuse. Examples of how NLOS configurations can work are presented in Figure 1.2.

**Reflective** links use the sea surface, where the beam is sent towards the sea surface. From there, the optical signal is further reflected towards the receiver facing the sea surface in a direction parallel to the reflected beam. In this way, an obstacle appearing in the path of the beam can be bypassed. The biggest problem is random phenomena on the surface of the water, which are changed by wind, sea currents, or other undesirable turbulences. Therefore, the beam can be reflected to the transmitter, which causes a high dispersion of the signal.

**Diffuse** links, as the name suggests, spread, or diffuse the optical beam to widen the FOV of the receiver. Sources can be lasers or high-power LEDs, and light propagation can serve as a broadcast from one source to multiple receivers. The main limitations are

short communication distances and lower transmission rates, as the scattered light is too attenuated over a large area of the water environment [1], [2].

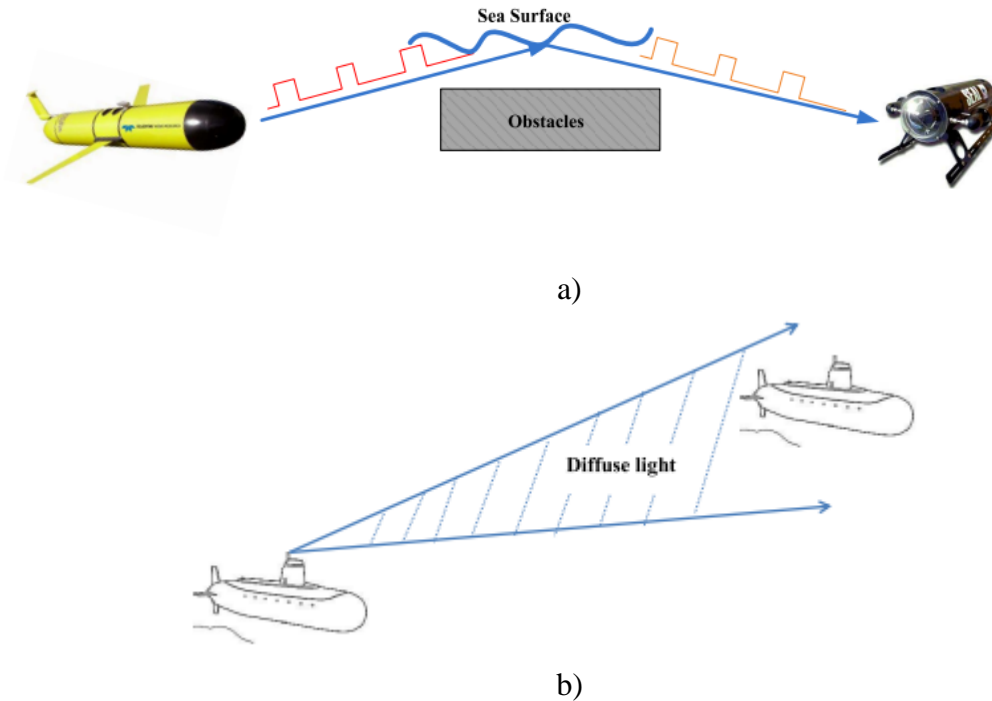


Fig. 1.2 NLOS configuration a) reflective (taken from [2]) and b) diffuse (taken from [1])

### 1.2.3 Retro-reflector links

The reflector configuration can be considered a special modification of the LOS point-to-point link. It is mostly used in duplex communication; receivers have limited power and weight budget. The beam source has a much larger power capacity and payload capacity than the receiver, thus serving as an interrogator that sends a modulated beam toward the receiver. The receiver is equipped with a small modulated optical reflector, and the transmitted beam is reflected to the source when detected at the receiver. Figure 1.3 briefly shows how this configuration works.

The main problem of this configuration is that the reflected beam may interfere with the originally transmitted beam from the source, which leads to a decrease in the system's signal-to-noise ratio (SNR) and bit-error-rate (BER), plus the received optical signal will have additional attenuation since it passes through the underwater channel twice [1], [2].

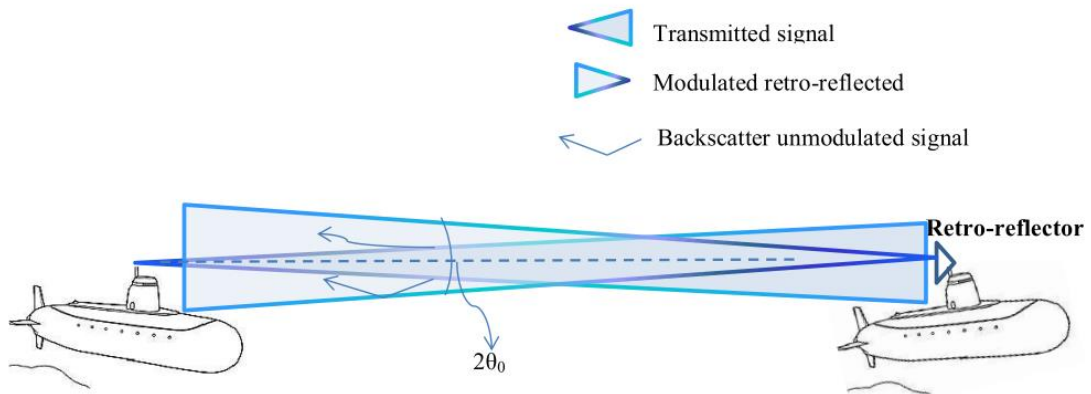


Fig. 1.3 Retro-reflection configuration (taken from [1])

### 1.3 Physical properties of the underwater medium

Because the basic characteristics of the underwater environment vary from shallow water to deep oceans, underwater light propagation is very sophisticated and challenging. The different properties of water media depend on the geographical location and the concentration of dissolved substances. In addition, different types of aquatic environments can also be generally divided into:

- 1) *Pure seawater*: Absorption is considered to be the main factor that limits the optical beam. It increases with increasing wavelength, which is why, for example, the red color with a wavelength of 500 nm is more attenuated than the blue color, and so deep clean oceans appear blue. Since the scattering coefficient is low to negligible, the beam propagates without divergence mainly in a straight line.
- 2) *Clear ocean water*: Dissolved particles such as salts, mineral components, colored dissolved organic matter, etc. are contained in higher concentrations in the oceans, and therefore the propagation of the optical beam is affected mainly by scattering.
- 3) *Coastal ocean water*: The effect of absorption and scattering will increase here, as the concentration of dissolved particles is even higher here. The main source of greater turbidity can be, for example, a high concentration of plankton, detritus, and minerals.
- 4) *Turbid harbor*: The attenuation of light propagation due to absorption and scattering is the greatest since turbid water contains the highest concentration of both, dissolved and suspended particles.

Furthermore, the optical properties of water can be divided into inherent optical properties and apparent optical properties. **Inherent properties** depend mainly on the composition of the medium and include the absorption, scattering, attenuation coefficient, and volume scattering function. They are typically used to determine the communication link budget in UOWC. On the other hand, the **apparent optical properties** depend on



both the medium and the geometric structure of illumination of diffused or collimated beams. They are mainly used for communication systems near the ocean's surface and evaluate the ambient light levels enabling their communication [1],[2].

Physical properties can also be further divided into zones according to vertical depth and light level. The upper layer is called the euphotic zone or sunlight zone and extends up to 200 meters. There is plenty of sunlight in this layer, so there is a high concentration of photosynthetic life, the presence of many marine mammals, and a large proportion of commercial fishing. The disphotic zone, where light intensity decreases with increasing depth, extends from 200 meters to 1000 meters. Since only a tiny amount of sunlight penetrates below 200 meters, photosynthesis cannot take place here. The zone into which no light ever penetrates is called aphotic and exists at depths below 1000 meters.[1], [3].

### 1.3.1 Factors affecting the UOWC

Several important factors have a major impact on UOWC. The two main coefficients that attenuate inherent properties are absorption and scattering. A simple geometric model is created for a simpler understanding of absorption and scattering, shown in Figure 1.4. Let us say that a volume of water  $\Delta V$  with thickness  $\Delta D$  is illuminated by a light beam of power  $P_I$  with wavelength  $\lambda$ , part of this light power is absorbed by the water and is denoted  $P_A$ , another part denoted  $P_S$  is scattered and the remaining power  $P_T$  that passed through the water is propagated as required. Therefore, according to the law of conservation of energy:

$$P_I(\lambda) = P_A(\lambda) + P_S(\lambda) + P_T(\lambda), \quad (1.1)$$

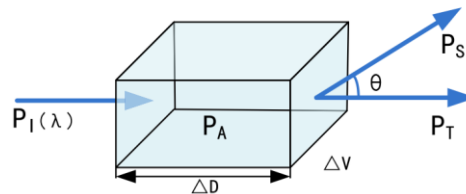


Fig. 1.4 Geometry of inherent optical property (taken from [2])

In general, **absorption** is a process of transferring energy where the energy of photons is lost and converted into other forms such as heat or chemicals (photosynthesis). The absorption in pure seawater is composed of water molecules and dissolved salts like NaCl, KCl, etc. As this environment is composed of these dissolved salts, a window will be created around the blue-green region of the visible spectrum, i.e. 400 nm - 500 nm, where absorption decreases.

The **scattering** effect is mainly dependent on the presence of various particles in the water; therefore, this phenomenon occurs more in coastal areas than in open oceans. When an optical beam passes through an environment that is affected by this phenomenon, it deviates from its original path, which leads to a reduction in the number

of photons at the receiver and a general reduction in the intensity of the received signal. Temperature, pressure, salinity, and other environmental changes also increase seawater dispersion.

In addition to absorption and scattering, other important factors such as beam spreading, turbulence, alignment, multipath interference, physical obstruction, and background noise need to be considered in the design and construction of UOWCs [1], [2].

Since this work is based on a non-attenuation environment, the calculation of refractive indices is not affected by the aforementioned unpredictable phenomena such as absorption and scattering, turbulence, etc.

### 1.3.2 Changes in temperatures in the aquatic environment

Temperature changes occur depending on depth, salinity, and pressure. In general, temperature decreases with increasing depth. As the aquatic environment was already divided into zones depending on the vertical depth and penetrating light, there is a layer called the thermocline at a depth of around 150 to 1000 meters. In this layer, the temperature drops rapidly depending on the increasing depth. The temperature is approximately the same from the surface up to about 100 meters, then decreases rapidly with increasing depth, and from around the area of 1000 meters and more the temperature decreases more slowly and settles at about 4 °C. For a simpler imagination, Figure 1.5 shows how the temperature changes depending on the increasing depth [4]. For higher latitudes, where surface temperatures are low, temperature changes minimally with increasing depth. For some very low temperatures in the thermocline, the temperature

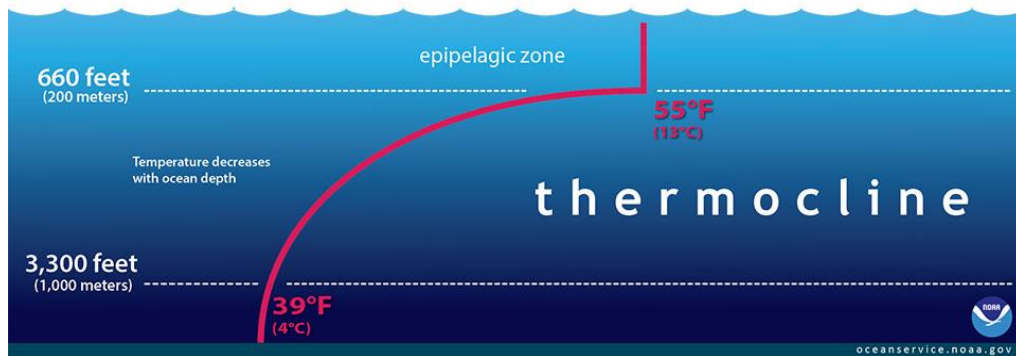


Fig. 1.5 Change of temperature with depth (taken from [4])

rises slightly. Therefore, if the temperatures are lower than 3 °C, the temperature is set as a constant. Also, if the specified depth is greater than 5000 meters, the temperature is set at a constant of 3°C and when the depth drops below 6500 meters and the temperature is below 3°C, the temperature is set to 2.5°C. Of course, the temperature in practice changes irregularly and various deviations may occur, therefore these simplifications are introduced to the calculations and set as constants for some extreme cases.

## 2. REFRACTIVE INDEX OF THE UNDERWATER MEDIUM

The refractive index is a dimensionless quantity that indicates the ratio of radiation propagation speed in a vacuum to the speed at which radiation propagates in a certain medium. A well-known relation for the general determination of the refractive index is:

$$n = \frac{c_0}{c}, \quad (2.1)$$

where  $n$  stands for the refractive index,  $c_0$  is the speed of radiation propagation in vacuum and  $c$  denotes the speed of radiation propagation in a certain medium. The refractive index defined in this way is called the absolute refractive index. In general, the index of refraction is a function of the type of substance, the density of the substance, and possibly the concentration of one substance in another, its value depends not only on the speed of propagation but also on the wavelength of the radiation that passes through a certain medium. Since the refractive index changes with different water environment conditions such as temperature, salinity, depth, and others, wavelength dependence is very important in UOWC. As changes in refractive index affect factors that have a significant impact on the UOWC, the windows of minimum absorption and scattering can be affected by these changes, thus, there is a significant advantage in choosing multi-wavelength links in a wavelength-dependent environment over choosing a single one.

The wavelength can further be expressed as the ratio between the speed of propagation of radiation in a certain environment  $c$  and the frequency  $\nu$ .

$$\lambda = \frac{c}{\nu}, \quad (2.2)$$

The relative index of refraction is arrangement-dependent and usually characterizes the interface properties of two optical media, unlike the absolute index, which is a material constant. Its relationship is thus derived as follows:

$$n_{12} = \frac{c_1}{c_2} = \frac{\frac{c_0}{n_1}}{\frac{c_0}{n_2}} = \frac{n_2}{n_1}, \quad (2.3)$$

where  $c_1$  and  $c_2$  is the speed of radiation propagation in two optical media [5].

## 2.1 General expression of refractive index

The index of refraction as the ratio of wave propagation speed in vacuum to that of a wave in a medium is derived as a constant from Maxwell's equations. In general, Maxwell's equations in a differential form describing the propagation of an electromagnetic wave are expressed by a system of equations:

$$\begin{aligned}
 \operatorname{div} \mathbf{B} &= 0, \\
 \operatorname{div} \mathbf{D} &= \rho_Q, \\
 \operatorname{rot} \mathbf{E} &= -\frac{\partial \mathbf{B}}{\partial t}, \\
 \operatorname{rot} \mathbf{H} &= \mathbf{j}_Q + \frac{\partial \mathbf{D}}{\partial t},
 \end{aligned} \tag{2.4}$$

where  $\rho_Q$  is bulk density and  $\mathbf{j}_Q$  volume charge density [6].

For the propagation of electromagnetic waves in a vacuum, the system of equations 2.4 can be simplified. Since there are no electric charges and currents,  $\rho_Q = 0, \mathbf{j}_Q = 0$ , and the material relations are of the form  $\mathbf{D} = \varepsilon_0 \mathbf{E}$  and  $\mathbf{B} = \mu_0 \mathbf{H}$ . Since the beam propagates in the direction of the energy flow, i.e., the direction of the so-called Poynting vector  $\mathbf{E} \times \mathbf{H}$ , the system of equations is modified using the following vectors:

$$\begin{aligned}
 \operatorname{div} \mathbf{H} &= 0, \\
 \operatorname{div} \mathbf{E} &= 0, \\
 \operatorname{rot} \mathbf{H} &= \varepsilon_0 \frac{\partial \mathbf{E}}{\partial t}, \\
 \operatorname{rot} \mathbf{E} &= -\mu_0 \frac{\partial \mathbf{H}}{\partial t},
 \end{aligned} \tag{2.5}$$

where  $\varepsilon_0 \approx 8,854 \cdot 10^{-12} \text{ F} \cdot \text{m}^{-1}$  is permittivity of vacuum and similarly  $\mu_0 \approx 4\pi \cdot 10^{-7} \text{ H/m}$  is permeability of vacuum. The components of both vectors  $\mathbf{E}$  and  $\mathbf{H}$  must satisfy the wave equation. The derivation of this equation for the  $\mathbf{E}$  component is achieved using a rotation operation that is applied to Maxwell's fourth equation 2.5:

$$\operatorname{rot} \operatorname{rot} \mathbf{E} = -\mu_0 \frac{\partial}{\partial t} (\operatorname{rot} \mathbf{H}) \rightarrow (\operatorname{grad} \operatorname{div} - \nabla^2) \mathbf{E} = -\mu_0 \frac{\partial}{\partial t} (\operatorname{rot} \mathbf{H}),$$

since  $\operatorname{div} \mathbf{E} = 0$  and  $\operatorname{rot} \mathbf{H} = \varepsilon_0 \frac{\partial \mathbf{E}}{\partial t}$ , [6], the resulting wave equation is:

$$\nabla^2 \mathbf{E} - \frac{1}{c^2} \frac{\partial^2 \mathbf{E}}{\partial t^2} = 0, \tag{2.6}$$

while the speed of wave propagation in vacuum  $c$  is:

$$c_0 = \frac{1}{\sqrt{\varepsilon_0 \mu_0}}. \quad (2.7)$$

Analogously, the wave equation for the vector  $\mathbf{H}$  can be derived from Maxwell's third equation from system 2.5:

$$\nabla^2 \mathbf{H} - \frac{1}{c^2} \frac{\partial^2 \mathbf{H}}{\partial t^2} = 0 \quad (2.8)$$

[6]. Since the speed of wave propagation in a certain medium is given as the quotient of the speed of wave propagation in a vacuum and the given medium:

$$c = \frac{c_0}{n}, \quad (2.9)$$

and, as the inverse of the square root of permittivity and permeability:

$$c = \frac{1}{\sqrt{\varepsilon \mu}}, \quad (2.10)$$

the refractive index is defined as:

$$n = \sqrt{\varepsilon_r \mu_r}. \quad (2.11)$$

### 2.1.1 Calculation of the refractive index

When counting the index for seawater it may be considered as a function of the salinity  $S$ , temperature  $T$ , pressure  $P$ , and wavelength  $\lambda$ . As already mentioned, this work deals with a non-attenuated aquatic environment, so pressure is not considered. In practice, these mentioned quantities change depending on the surrounding conditions, and from an oceanographic point of view, the following ranges are relevant:  $0 < S < 43$  ‰,  $0 < T < 30$  °C. The important range for wavelength is  $400 < \lambda < 700$  nm, which is the visible spectrum [7].

In this work, the counting of the refractive index is based on the empirical equation proposed in [8]:

$$n = aT^2 + b\lambda^2 + cT + d\lambda + e, \quad (2.12)$$

where  $a$ ,  $b$ ,  $c$ ,  $d$ , and  $e$  are coefficients that vary with salinity. The values of these coefficients are shown in the following table.

Table 2.1 Table of coefficient values for fresh and saltwater (taken from [8])

<b>Coefficient</b>	<b>Seawater (S = 35 ‰)</b>	<b>Freshwater (S = 0 ‰)</b>
<i>a</i>	$-1.50156 \times 10^{-6}$	$-1.97812 \times 10^{-6}$
<i>b</i>	$1.07085 \times 10^{-7}$	$1.03223 \times 10^{-7}$
<i>c</i>	$-4.27594 \times 10^{-5}$	$-8.58125 \times 10^{-6}$
<i>d</i>	$-1.60476 \times 10^{-4}$	$-1.54834 \times 10^{-4}$
<i>e</i>	1.39807	1.38919

The equation (2.13) depends on temperature and wavelength, and on salinity that varies for freshwater and seawater. For freshwater, the salinity is  $S = 0 \text{ ‰}$  and for seawater, the salinity is  $S = 35 \text{ ‰}$ , as can be seen in Table 2.1, and therefore the refractive index calculations implemented in the program work with salinity as a constant [8].

## **3. WORLD MAP MODELLING**

### **3.1 Program parameters**

The main goal was to create a program that will be able to determine the index of refraction of the underwater environment for the specified input parameters, display the profile of the index of refraction of the water environment between two points, which are determined by geographical coordinates and the depth below the water surface, and based on this profile on the given route, display the propagation of the optical bundle of suitable wavelengths.

The purpose of the program is to understand the changes in the refractive indices in the water environment for the possible propagation of information through the water medium, as these changes are important for setting up transmitters and receivers. Since the transmitters are radiation sources such as LED radiation or lasers, the choice of a suitable wavelength is very important, as the refractive index of the water environment changes for different wavelengths which has a significant impact on the beam propagation in the underwater medium.

The input of this program is suitably selected geographical coordinates, depth below sea level or the choice of salinity. Input parameters are also values in the form of datasets, available online, which are sea surface temperatures and maximum possible depth. The output is changes in the local refractive index of the water environment and the refractive index on the route between two points, which affect the propagation of optical beams, and the display of propagation changes on the route.

The program was created using the Python programming language. This language was chosen because it is becoming more and more popular recently, it is very adaptable, and it is not difficult to learn. One of the big advantages is a very extensive library, it also enables faster and slightly easier creation of graphical user interfaces thanks to many built-in tools.

Figure 3.1 shows a flowchart of the entire program that briefly describes its function.

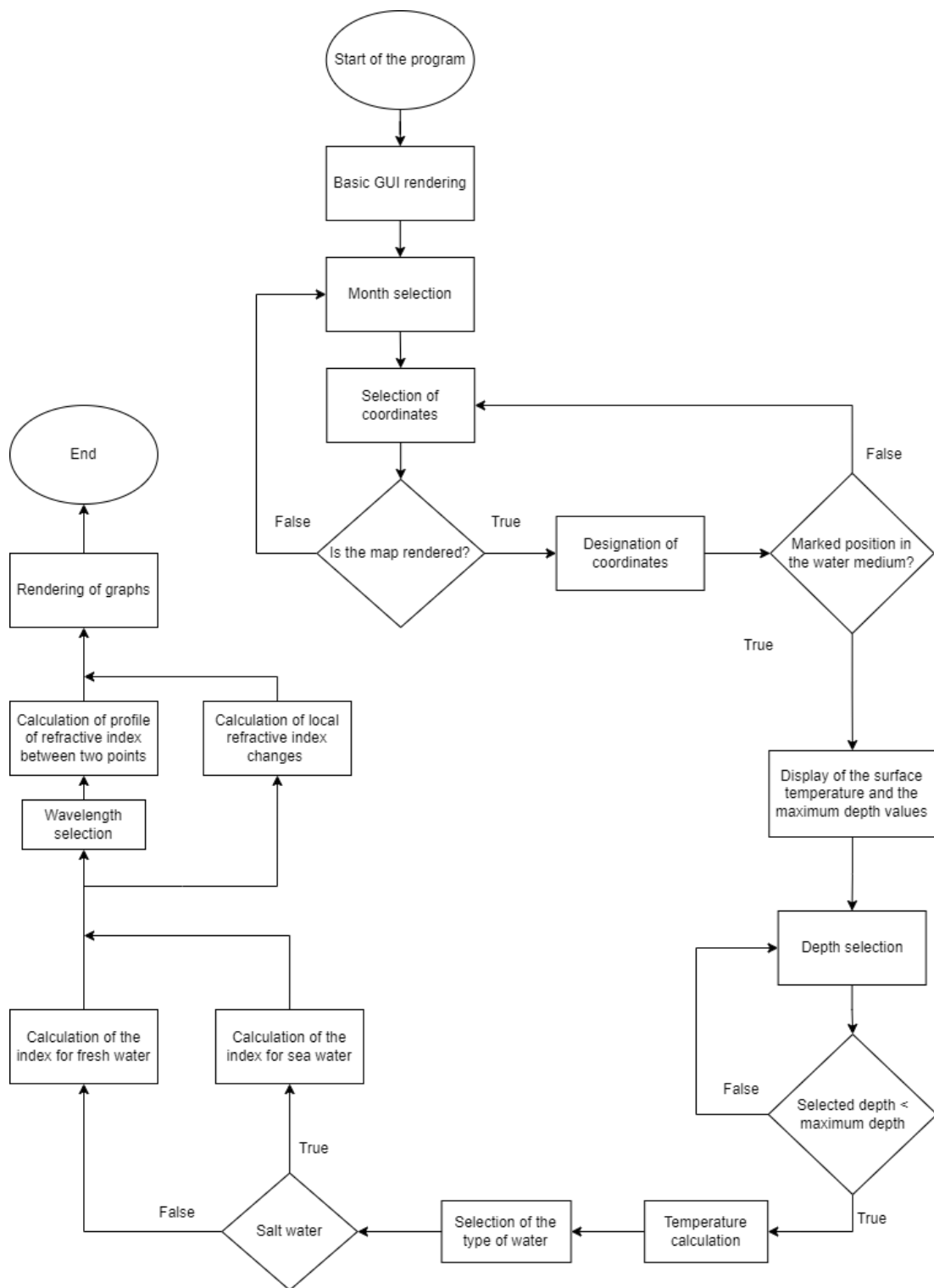


Fig. 3.1 Flowchart diagram of program function



### 3.1.1 Input parameters

As input parameters, user-selected coordinates are entered into the program as *DDM* (Degrees with Decimal Minutes) format values, which means longitude ranges from 0° to 180° and latitude ranges from 0° to 90°. Another parameter is the depth, which is limited using the dataset consisting of bathymetry data which is a digital image of the undersea surface and water depth, then the temperature corresponding to the specified depth. And finally, the choice of salinity between fresh and salt water.

Sea surface temperature datasets were used for the year 2021 for January to December [9] and the downloaded bathymetry dataset corresponds to the year 2002 [10].

## 3.2 Structure and function of the program

As mentioned, Python language was used to create a program for drawing a world map. Figure 3.2 is an example of how the main window of the created program might look like. Individual parts will be described in more detail.

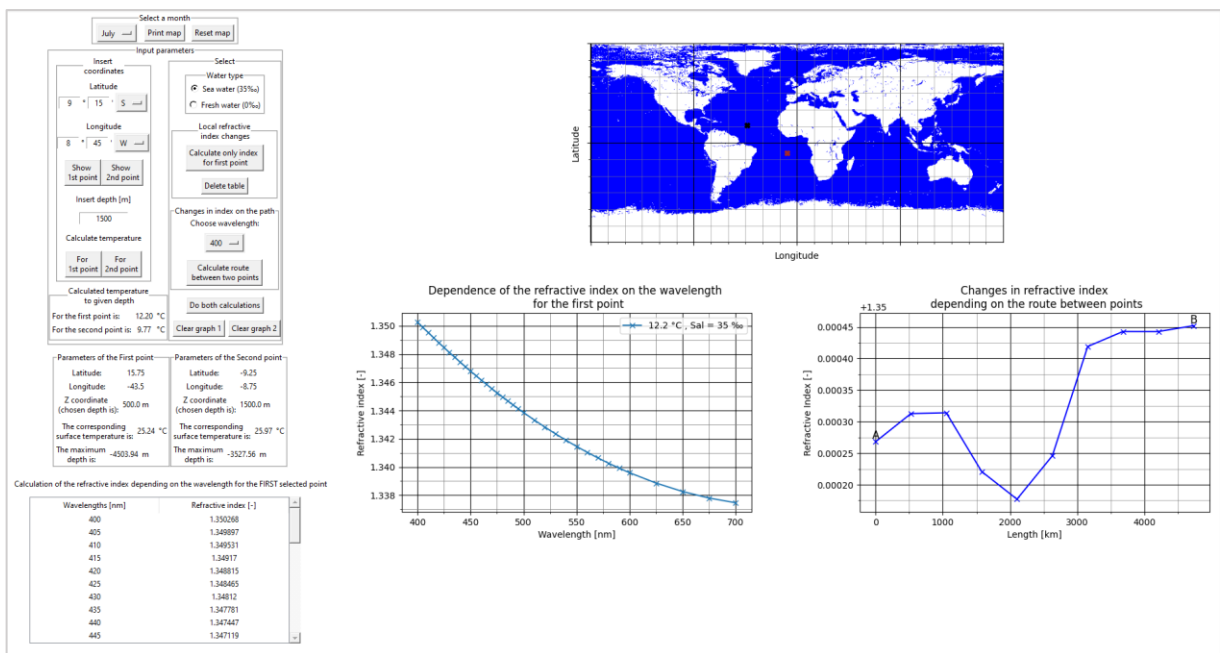


Fig. 3.2 An example of how the main program looks

First, after running the code, the skeleton of the program is rendered, which are only the basic elements of the Graphical User Interface (GUI). Figure 3.3 shows how the program looks after starting. In this part, the program loads the downloaded depth datasets used later in the calculation of temperatures and indices.

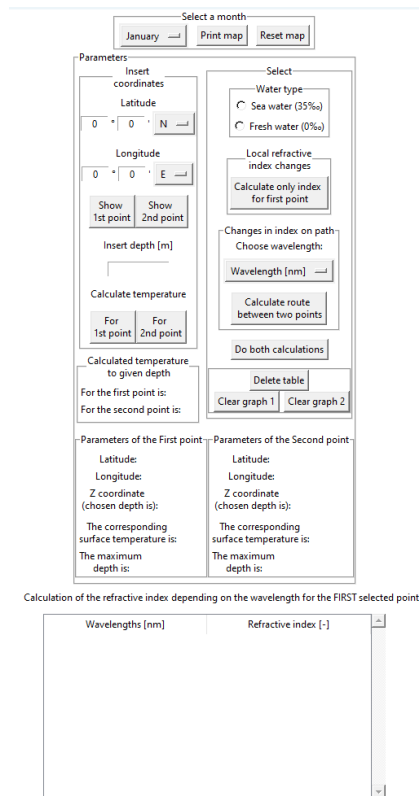


Fig. 3.3 The main window of the program after the startup  
For better representation, this panel will subsequently be described in parts.

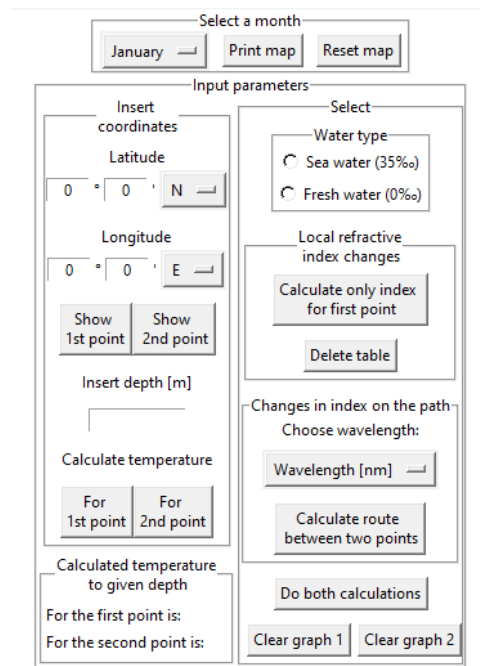


Fig. 3.4 The first part of the main panel

Figure 3.4 shows the main part where the user chooses the input parameters. In the “Select a month” section, the user is given a choice from all 12 months, and after selecting one, the user draws a map that contains the values of the surface temperatures of the oceans and seas, which differ for the given months and therefore each drawn map differs in appearance. The “Input parameters” section can be divided into three parts. The first part “Insert coordinates” serves to select two different points (transmitter and receiver). Each point is drawn on the map using its buttons. The “Calculated temperature to given depth” part shows the user a calculated temperature of each point in the selected depth, calculated by its buttons as well. And in the third part “Select”, the user chooses the salinity of the water environment and whether he wants to calculate the change in the local refractive index of the transmitter, the change in the refractive index on the path between the transmitter and the receiver, or both calculations at once. The user chooses wavelengths in the range of 400 nm to 700 nm.

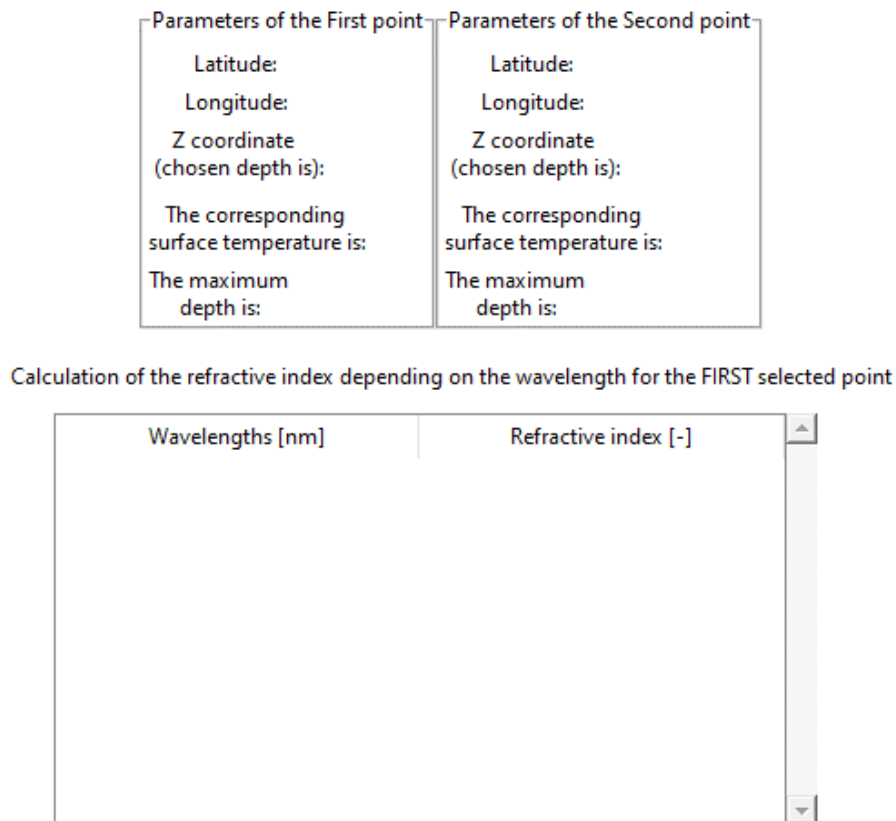


Fig. 3.5 The second part of the main panel

Figure 3.5 consists of two parts. In the upper part, there are individual parameters of the selected points. The selected coordinates and depth are displayed here, followed by the corresponding surface temperature and maximum depth at the given point. In the

lower part, there is a table that contains the calculated values of the refractive indices of the transmitter for different wavelengths.

Furthermore, as already mentioned, after selecting a month, a map is drawn in the right part of the program, which contains a dataset of surface temperature. Figure 3.6 shows an example of how the map is drawn for the month of January.

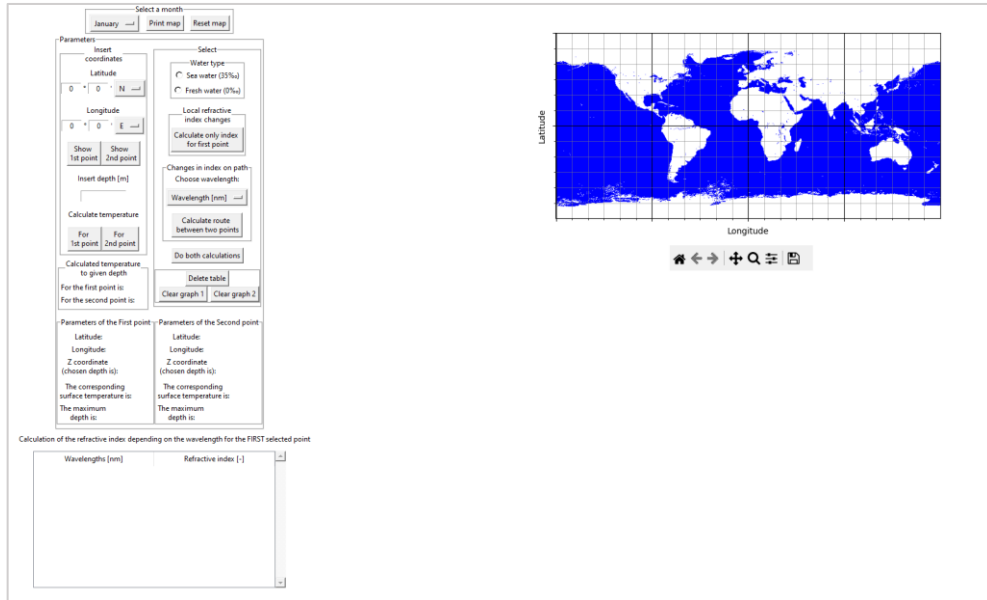
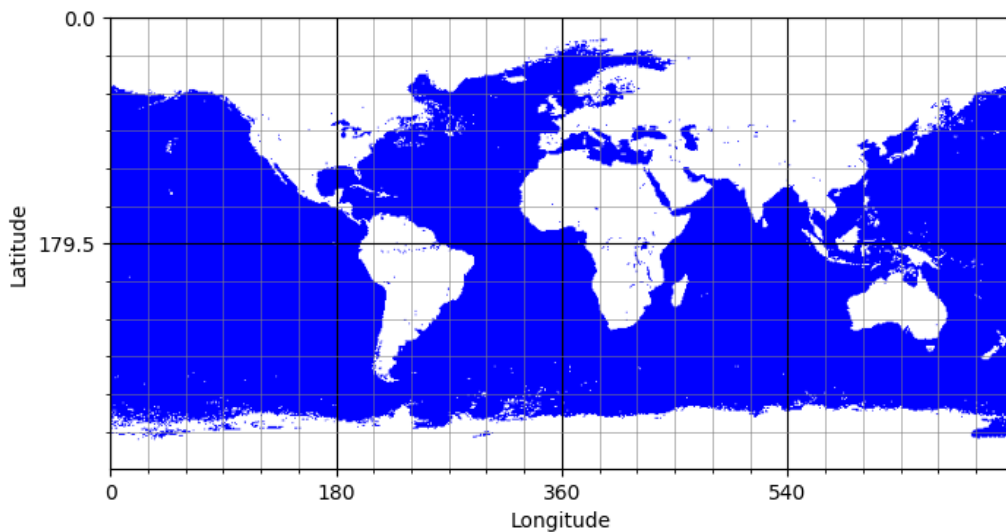
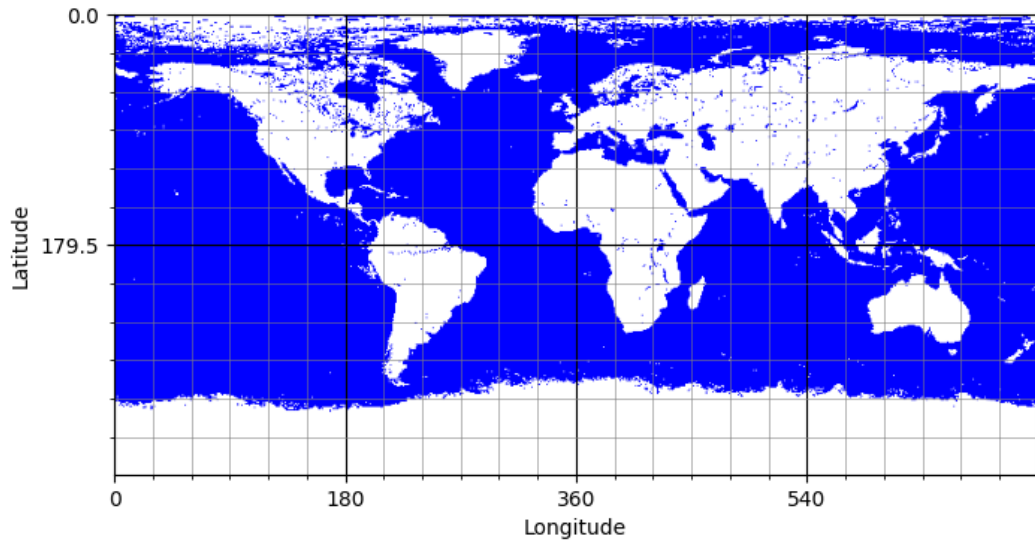


Fig. 3.6 Program after selecting the map (January)

A closer look at the created maps in Figure 3.7 can be seen, a) a map for the month of February and b) a map for the month of August.



a)



b)

Fig. 3.7 Detailed image of rendered maps for a) February, and b) August

Detailed Figure 3.7 shows how the sea surface temperature has changed during the year with the water surface freezing in the Northern Hemisphere during the winter months and in the Southern Hemisphere during the summer months. The map is drawn with an accuracy of 0.5 degrees, and the size of the image according to the Excel file is 720x360 pixels.

Select a month: January Print map Reset map

**Input parameters**

**Insert coordinates**  
 Latitude: 40 ° 30 ' N  
 Longitude: 40 ° 15 ' W  
Show 1st point Show 2nd point

Insert depth [m]:  
 Calculate temperature:  
 For 1st point For 2nd point

Calculated temperature to given depth:  
 For the first point is:  
 For the second point is:

**Parameters of the First point**  
 Latitude: 40.25  
 Longitude: -30.75  
 Z coordinate (chosen depth is):  
 The corresponding surface temperature is: 15.92 °C  
 The maximum depth is: -2519.69 m

**Parameters of the Second point**  
 Latitude: 40.5  
 Longitude: -40.25  
 Z coordinate (chosen depth is):  
 The corresponding surface temperature is: 17.96 °C  
 The maximum depth is: -4881.89 m

**Select**  
 Water type  
 Sea water (35%)  
 Fresh water (0%)

Local refractive index changes:  
Calculate only index for first point  
Delete table

Changes in index on the path:  
 Choose wavelength:  
 Wavelength [nm]:  
Calculate route between two points  
Do both calculations  
Clear graph 1 Clear graph 2

a)

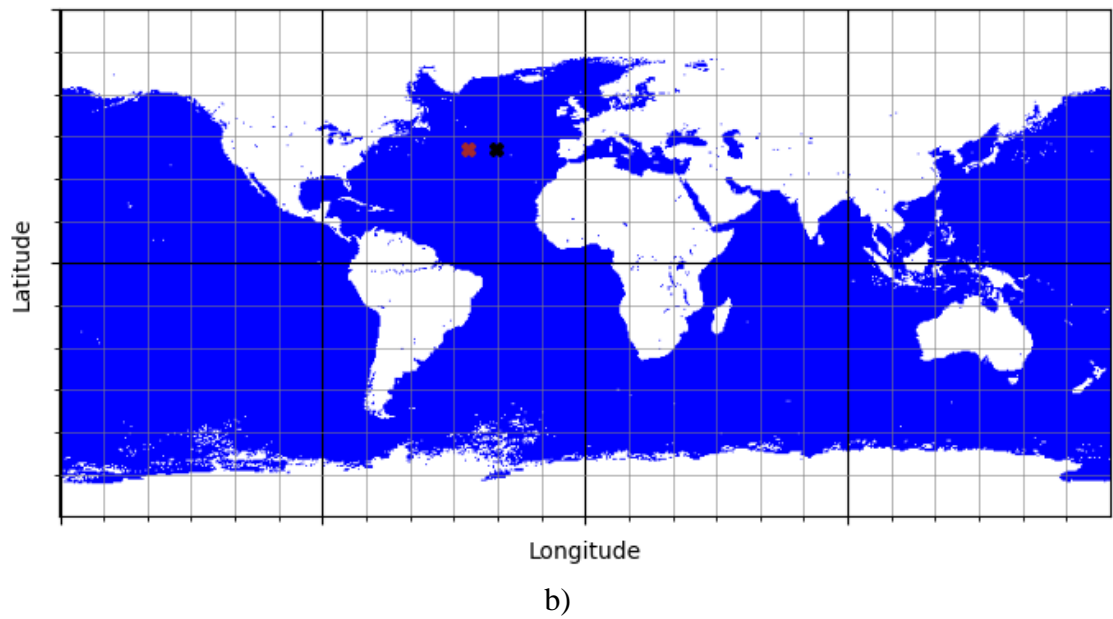


Fig. 3.8 a) Program after inserting the coordinates, b) detailed view of the map

Figure 3.8 shows how the points are displayed on the map after entering the coordinates for both points. The black cross represents the first point (transmitter), and the brown cross represents the second selected point (receiver). Coordinates of the first point are  $40^{\circ}15' \text{ N}$ ,  $30^{\circ}45' \text{ W}$  and the coordinates of the second point are  $40^{\circ}30' \text{ N}$ ,  $40^{\circ}15' \text{ W}$ . Thus, the coordinates are selected in DDM format and then converted to DD (Decimal Degrees) format.

After the coordinates were selected, it is possible to calculate the temperature at the given depth. The above-mentioned coordinates for individual points will be used for the demonstration.

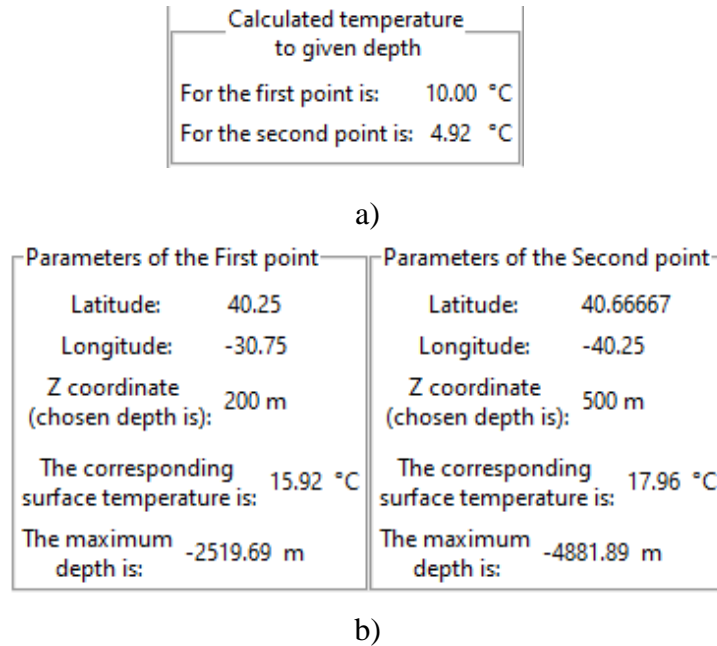


Fig. 3.9 a) An example of calculated temperatures, b) Parameters of the selected point

As shown in Figure 3.9, the temperature at a certain depth was calculated for two selected points. The determined coordinates were converted to DD format and displayed below in “Parameters” for each point. Here you can also see the selected depths and the corresponding surface temperature of the water and the maximum depth at the given point, in this case, 200 meters for the First point and 500 meters for the Second point. Please note that even though the maximum depth is a negative value, the selected depth is entered as positive.

After choosing all these necessary parameters, the user can proceed to the calculations of the refractive indices themselves, which are done with the following buttons.

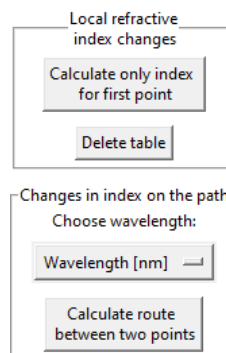


Fig. 3.10 Buttons for calculating refractive indices

### 3.2.1 Local refractive index of the transmitter for different wavelengths

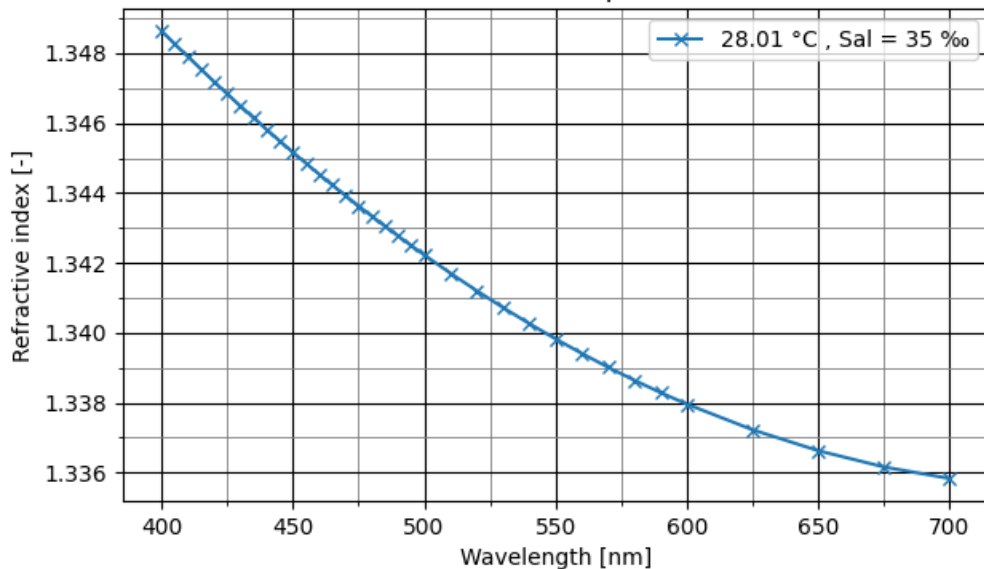
While the refractive indices are calculated and written in the table, a graph of the dependence of the refractive indices on certain wavelengths is drawn below the map. The point  $0^{\circ} 0' N, 0^{\circ} 0' E$  was selected with a chosen depth of 20 meters. The calculations were performed using the equation presented in [8], whose input parameters are wavelength and temperature at a given depth in the range of 0 - 30 °C. Figure 3.11 shows an example of how the refractive index can change.

Calculation of the refractive index depending on the wavelength for the FIRST selected point

Wavelengths [nm]	Refractive index [-]
400	1.348637
405	1.348266
410	1.3479
415	1.347539
420	1.347184
425	1.346834
430	1.34649
435	1.34615
440	1.345816
445	1.345488

a)

Dependence of the refractive index on the wavelength for the first point



b)

Fig. 3.11 Dependence of the refractive index on wavelengths for a temperature of 28.01 °C, a) calculated values in the table, b) calculated values in the graph



Figure 3.12 serves as an example of how the refractive index changes with depth and temperature. A surface temperature of 28.01 °C corresponds to a depth of 20 meters, a blue curve, and a depth of 4500 meters corresponds to 10.76 °C, an orange curve.

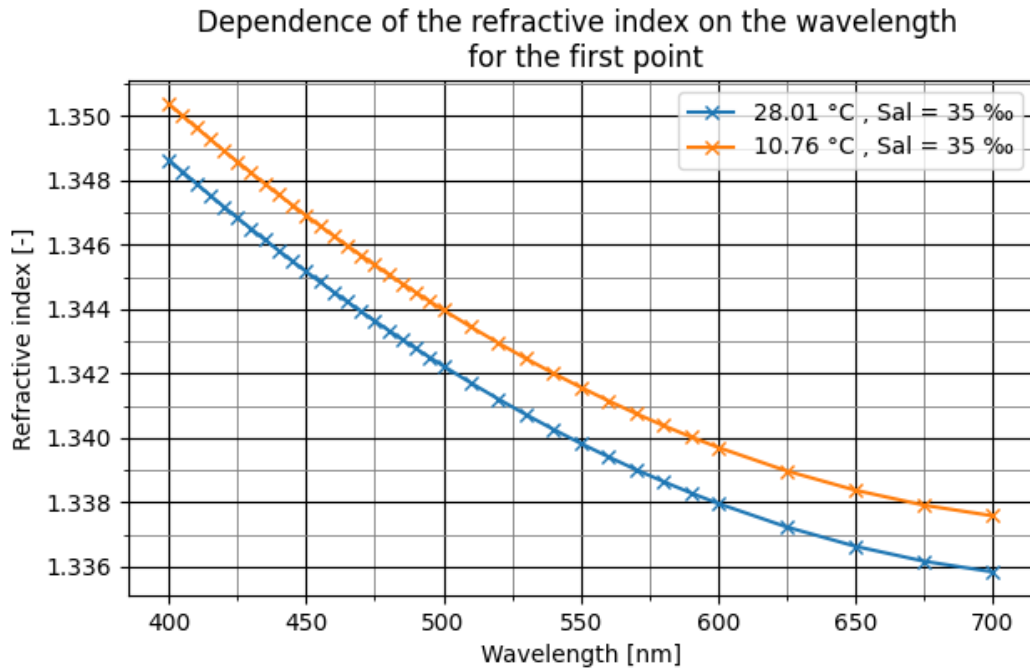


Fig. 3.12 Dependence of the refractive index on wavelengths for a temperature of 28.01 °C and 10.76 °C

From these graphs in Figures 3.11 and 3.12 follows that the refractive index decreases with increasing wavelength and decreases with increasing temperature. The decline is approximately linear for wavelengths between 400 nm and 500 nm, after which it begins to decline slightly non-linearly. These calculations were made for seawater with a salinity equal to  $S = 35 \text{ ‰}$ .

Figure 3.13 shows an illustrative example of how the refractive index changes for different salinities. The refractive index is calculated at the same depth of 20 meters for the same temperature of 28.01 °C, but with different salinity. For the blue curve, the salinity value is  $S = 35 \text{ ‰}$  and for the orange curve, the salinity value is  $S = 0 \text{ ‰}$ . The refractive index also increases with increasing salinity.

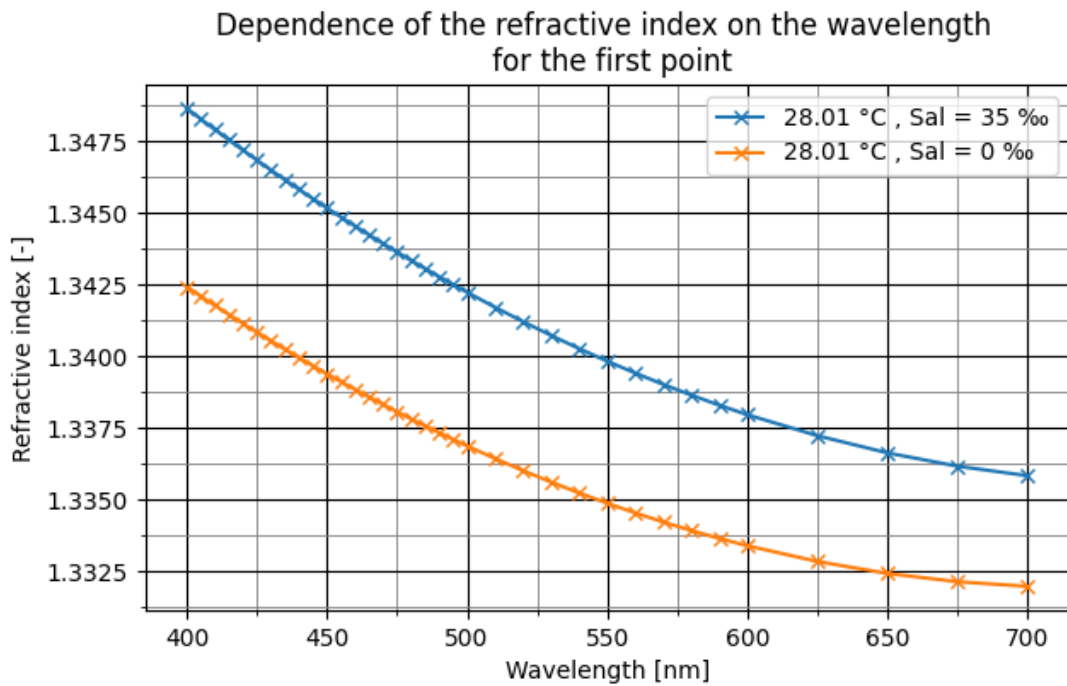


Fig. 3.13 Dependence of the refractive index on wavelengths for a temperature of 20.00 °C for different salinities

And lastly, a comparison of refractive indices for salinity  $S = 0 \text{ ‰}$  for different temperatures at different depths is displayed in Figure 3.14. As already shown in Figure 3.12 for seawater, the refractive index increases with the decreasing temperature, and in general, the refractive index for fresh water is lower than for salt water. As an example, only for fresh water, in Figure 3.14 refractive indices are calculated for temperatures 28.01 °C and 10.76 °C, at  $S = 0 \text{ ‰}$ .

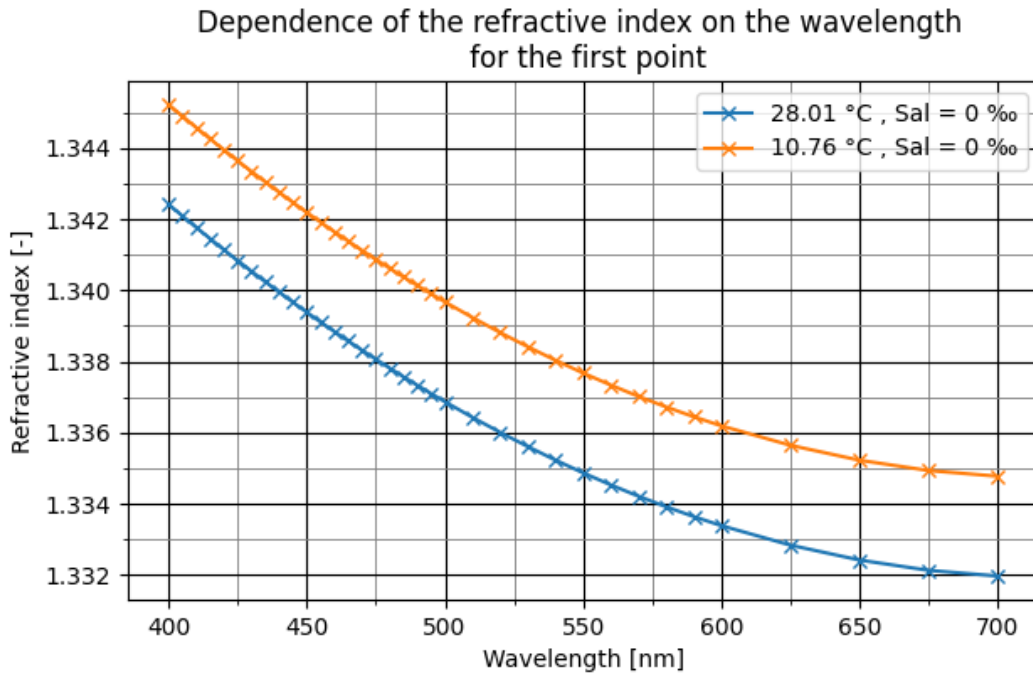


Fig. 3.14 Dependence of the refractive index on wavelengths for a temperature of 20.00 °C and 3.5 °C for freshwater

### 3.2.2 Changes in refractive index on the path between two points

Changes in the water medium temperature are used to calculate changes in refraction indices along the path between two points. Each temperature corresponds to a certain index of refraction, which divides the environment into individual layers. The route between two selected points is divided along its entire length into several intermediate steps, for which the angle, at which the beam enters the next layer, is calculated in the individual layers. The well-known Snell's law is used for these calculations.

$$n_1 \sin \theta_1 = n_2 \sin \theta_2, \quad (3.1)$$

Since the angle at which the beam hits the next layer is determined, Snell's law is adjusted to the following form:

$$\theta_2 = \sin^{-1} \left( \frac{n_1}{n_2} \sin \theta_1 \right), \quad (3.2)$$

where  $n_1$  and  $n_2$  correspond to the refractive indices of individual layers, and  $\theta_1$  and  $\theta_2$  are the angles of beam propagation through the individual layers.

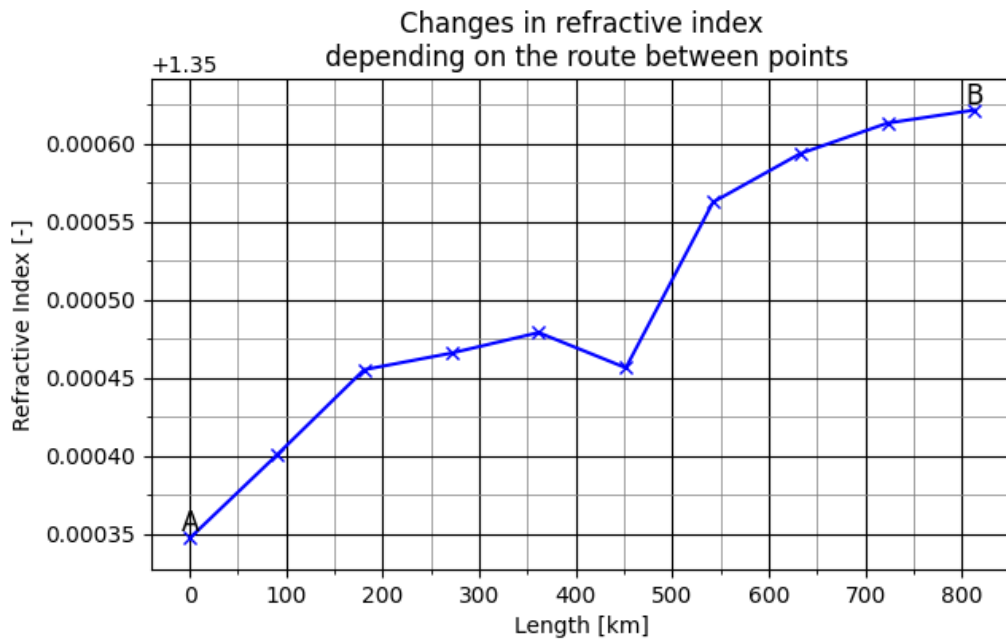


Fig. 3.15 Refractive index changes in the environment between two points

Figure 3.15 is an example of how the refractive index changes in the path between two points. The first point with the selected coordinates 36°45'N 39°00'W was located at a depth of 500 meters, with a corresponding temperature of 11.18°C. The coordinates of the second point are 39°45'N 47°30'W at a depth of 1500 meters and with a temperature of 7.29°C. The refractive index varies in the range of 1.35034 to 1.35065 and it increases as the temperature of the water medium decreases. A map for the month of July was used for these calculations and the wavelength was set to 400 nm.

Calculated temperature to given depth	
For the first point is:	11.18 °C
For the second point is:	7.29 °C

Parameters of the First point	Parameters of the Second point
Latitude: 36.75	Latitude: 39.75
Longitude: -39.0	Longitude: -47.5
Z coordinate (chosen depth is): 500.0 m	Z coordinate (chosen depth is): 1500.0 m
The corresponding surface temperature is: 24.22 °C	The corresponding surface temperature is: 23.49 °C
The maximum depth is: -3559.06 m	The maximum depth is: -3905.51 m

Fig. 3.16 Parameters of the First and the Second point

The parameters of both points are shown in Figure 3.16.

In an ideal environment, the beam would propagate between these points without any change, but in this case, due to these changes in the refractive index, the beam does not propagate directly, resulting in a deflection from the original point. For the case in Figure 3.15, where the refractive index increases almost all the time, the deviation is shown in Figure 3.17.

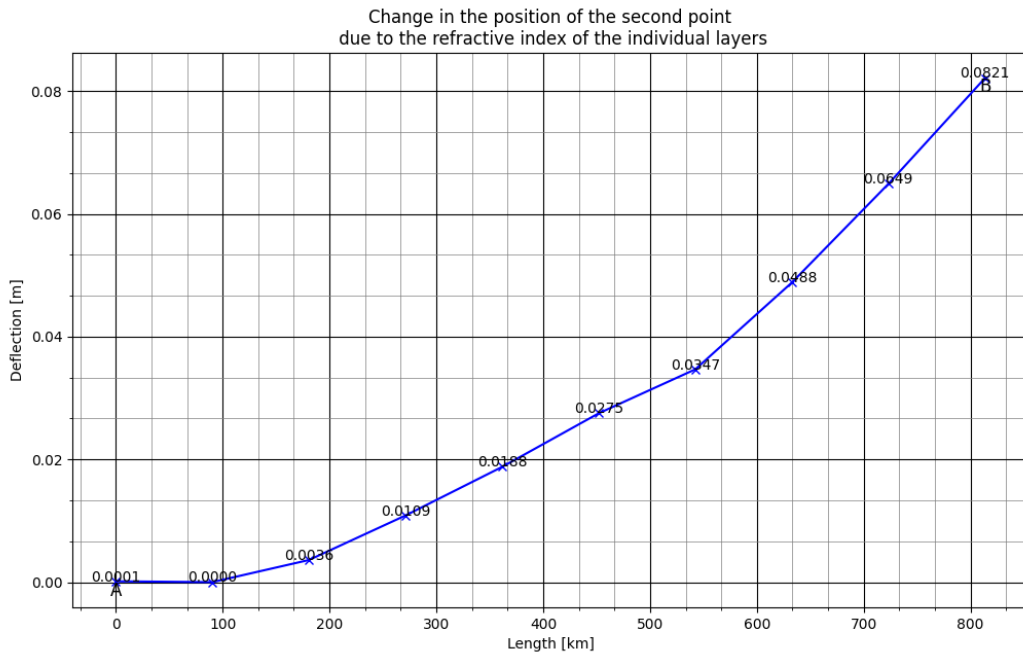
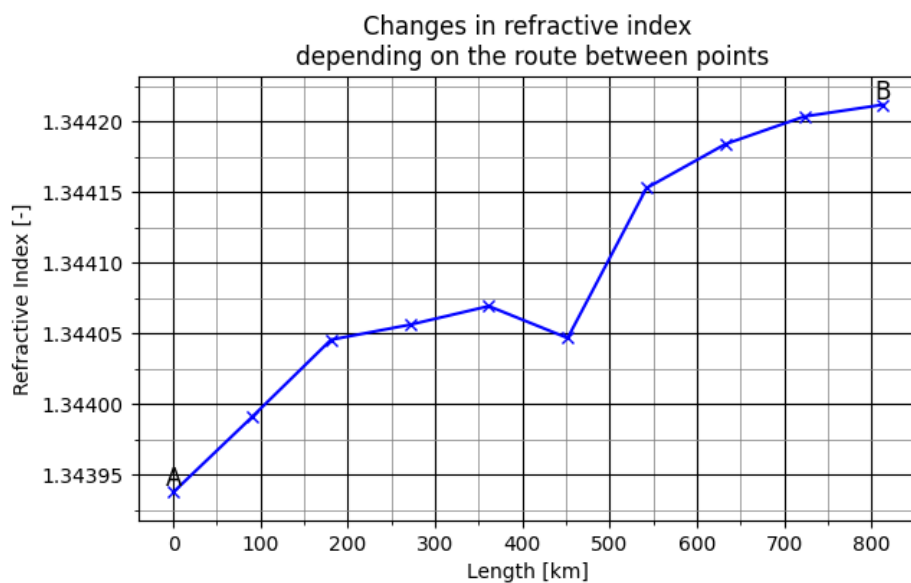
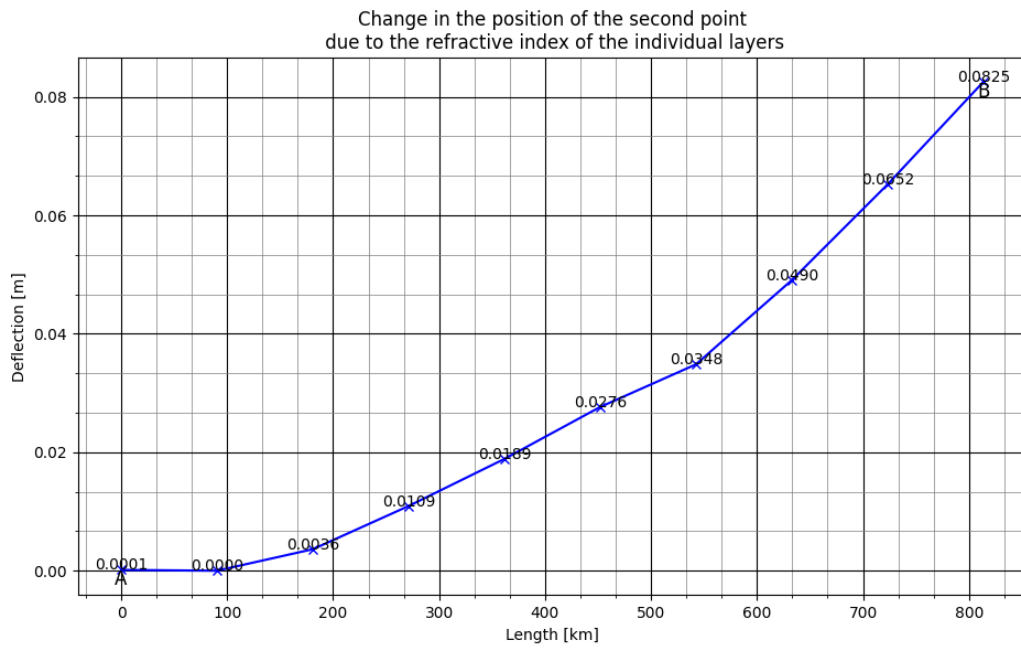


Fig. 3.17 Beam spreading deflection

The consequence of these changes is a deviation of the propagation of the optical beam from the original point in this case by 0.0821 meters.



a)

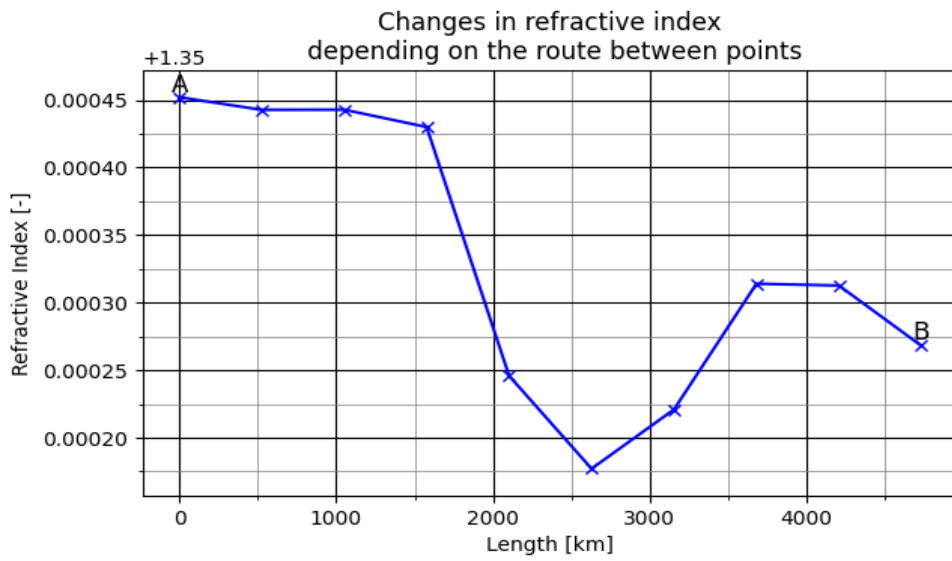


b)

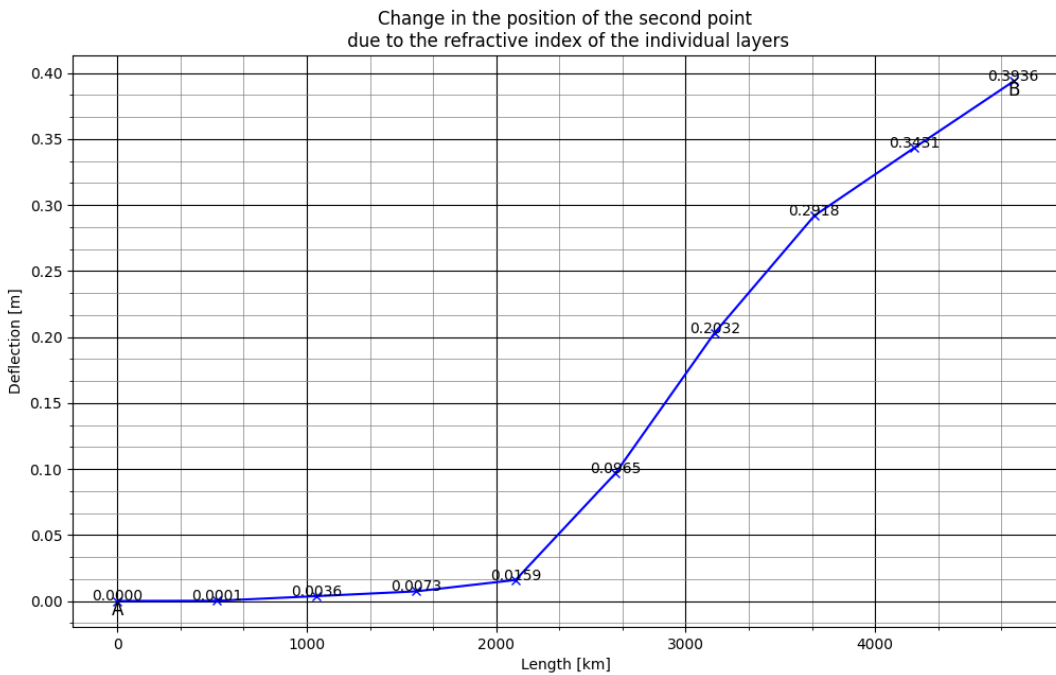
Fig. 3.18 Beam spreading deflection for different wavelength

For the case in Figure 3.18, the wavelength has been resized to 500 nm for the same two points. The spread of the refractive index shifted to the range of 1.34390 - 1.34425, so as the wavelength increased, the refractive index decreased and thus the deviation values increased when in this case point B is deflected by 0.0825 meters.

In terms of reciprocity, these systems are non-reciprocal. Changes in the index of refraction affect the beam so that if it propagates in one direction somehow, it will not propagate the same way in the opposite direction. Two points with different coordinates are chosen as an example, for the first point the coordinates are 9°15'S 8°45'W and the depth is 1500 meters, the second point is in the place with the coordinates 15°45'N 43°30'W, 500 meters below the surface.



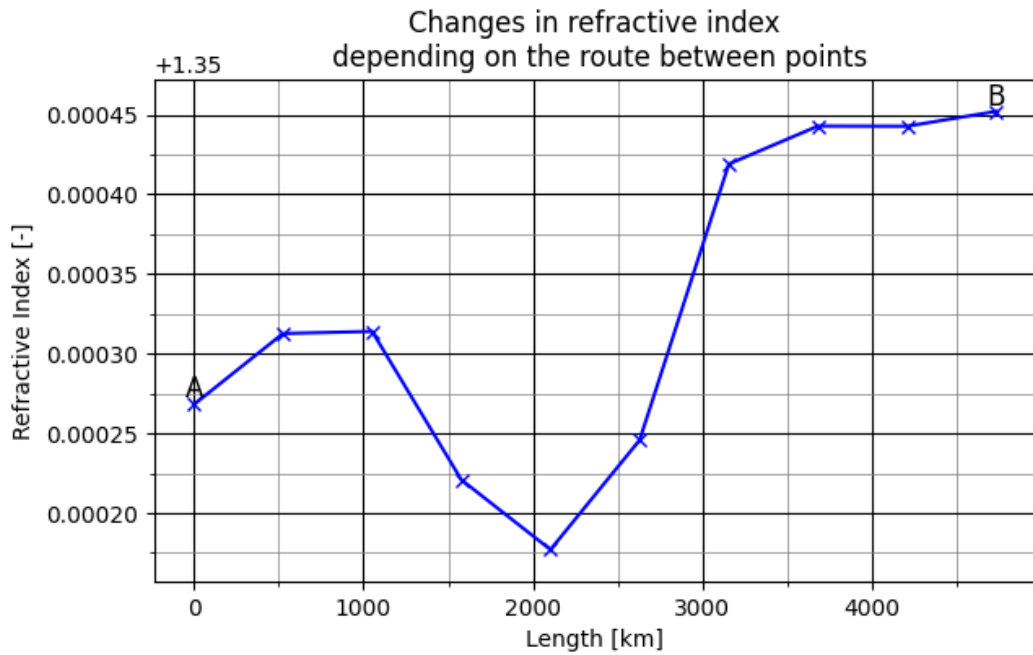
a)



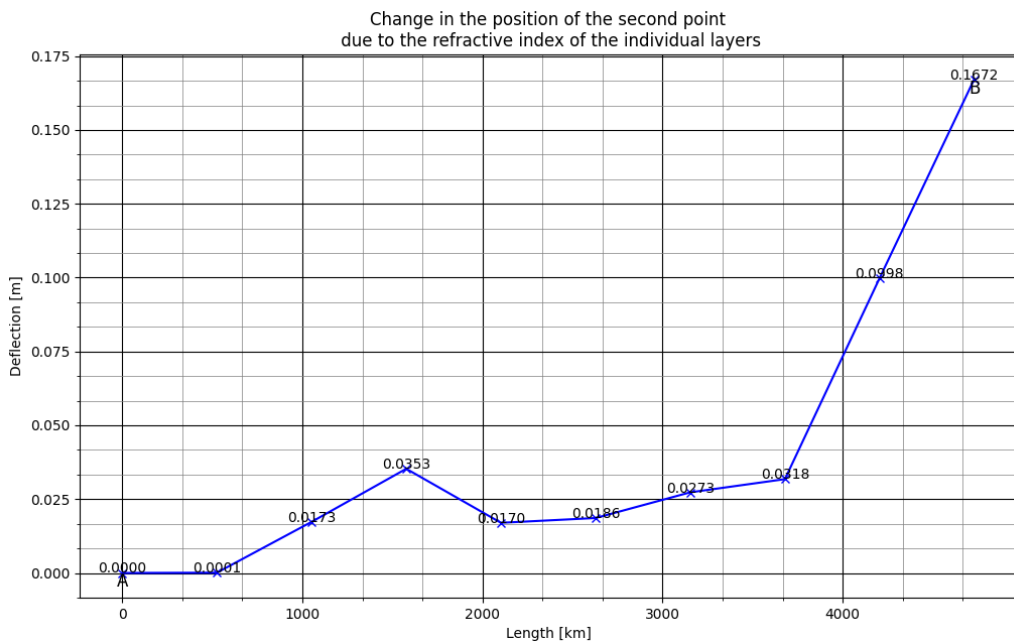
b)

Fig. 3.19 Forward propagation as an example of non-reciprocity

Figure 3.19 shows how the index of refraction spreads and how the second point deviates, the deviation of point B is 0.3936 meters. For counting map of July was printed and a wavelength of 400 nm was selected. But if we switch the two points so that the first point has the coordinates and depth of the second point and vice versa, the deviation is different and the graph of changes in the refractive index on this route is inverted.



a)



b)

Fig. 3.20 Reverse propagation as an example of non-reciprocity

Figure 3.20 perfectly shows the non-reciprocity, where after swapping points, the deviation of point B changed from the original value of 0.3936 meters to the value of 0.1672 meters. The graph of refractive index changes on the track uses the same intermediate points which are automatically calculated for the given length, so this graph is inverted. Each point is separated by a length that is determined by the ratio of the total length between the two selected points and the number of intermediate calculations.

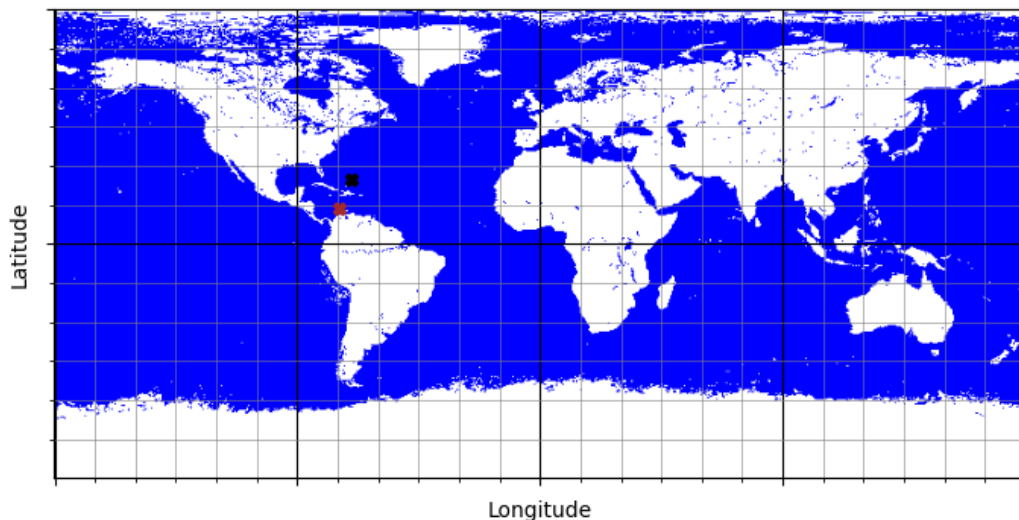


Figure 3.19a) and 3.20b) also offers an interesting view of how the refractive index of the underwater environment changes around the equator. As the temperature increases, the index of refraction decreases, which was significantly manifested in the vicinity of the equator, where there is rapid warming, due to, for example, the Gulf Stream, and thus the index of refraction decreases.

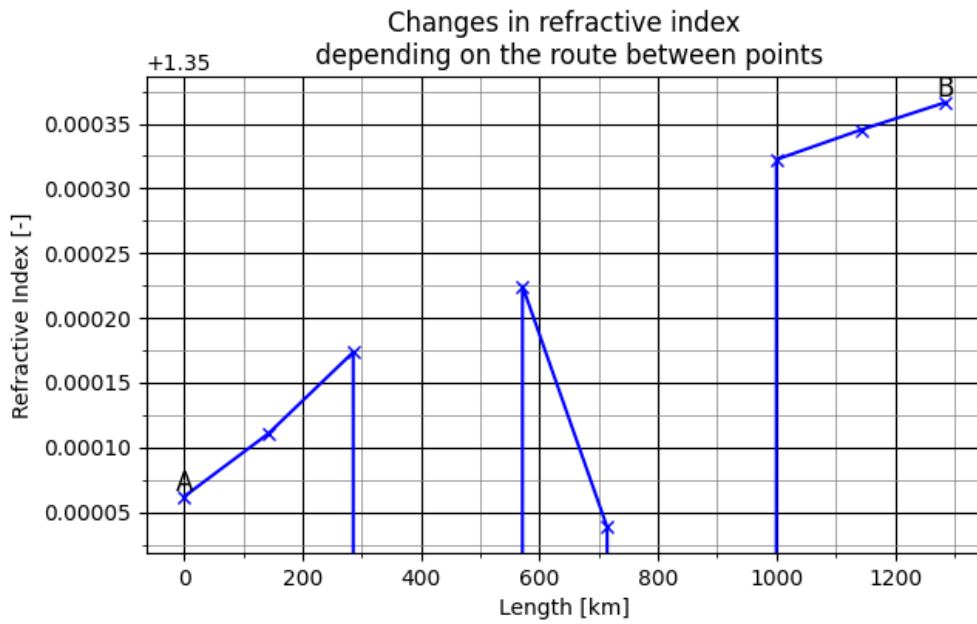
### 3.2.3 Beam spread over land and its length

Since optical wireless technologies are considered, the length of the beam propagation is very limited, however, the created program does not contain any length restrictions. In a real case, an unlimited beam length would be exceedingly difficult to achieve, though, by using additional sources, amplifiers, or underwater transceivers in the path between two points, a greater range of propagation could be achieved.

With an unlimited beam propagation length in the program, for example, the problem of beam propagation across continents arises. If two points are selected and land is detected between them, or the occurrence of some islands, the refractive index is automatically set to  $n = 1$ , and in the real case, the connection would be interrupted. By using auxiliary satellites or other transceivers, it would be possible to avoid breaking the connection between two points separated by land.



a)



b)

Fig. 3.21 Spreading the beam across the land a) A map for the month of July, b) a graph of how the refractive index changes on the path

Figure 3.21) is a map for the month of July and an example of choosing two points between which there is land. Figure 3.21b) is a graph of the change in refractive index on the way between these two points. As mentioned, the indices that correspond to the land site are set to  $n = 1$ , so there are steep falls to this value in this graph, but the y-axis has been limited to keep the appropriate range of the refractive index of the aquatic environment.

As a result of these changes, the deviation values are very imprecise, and we can get results like in Figure 3.22. In this graph, two transitions between land and water can be seen, resulting in a deviation of the second point by more than 100 meters.

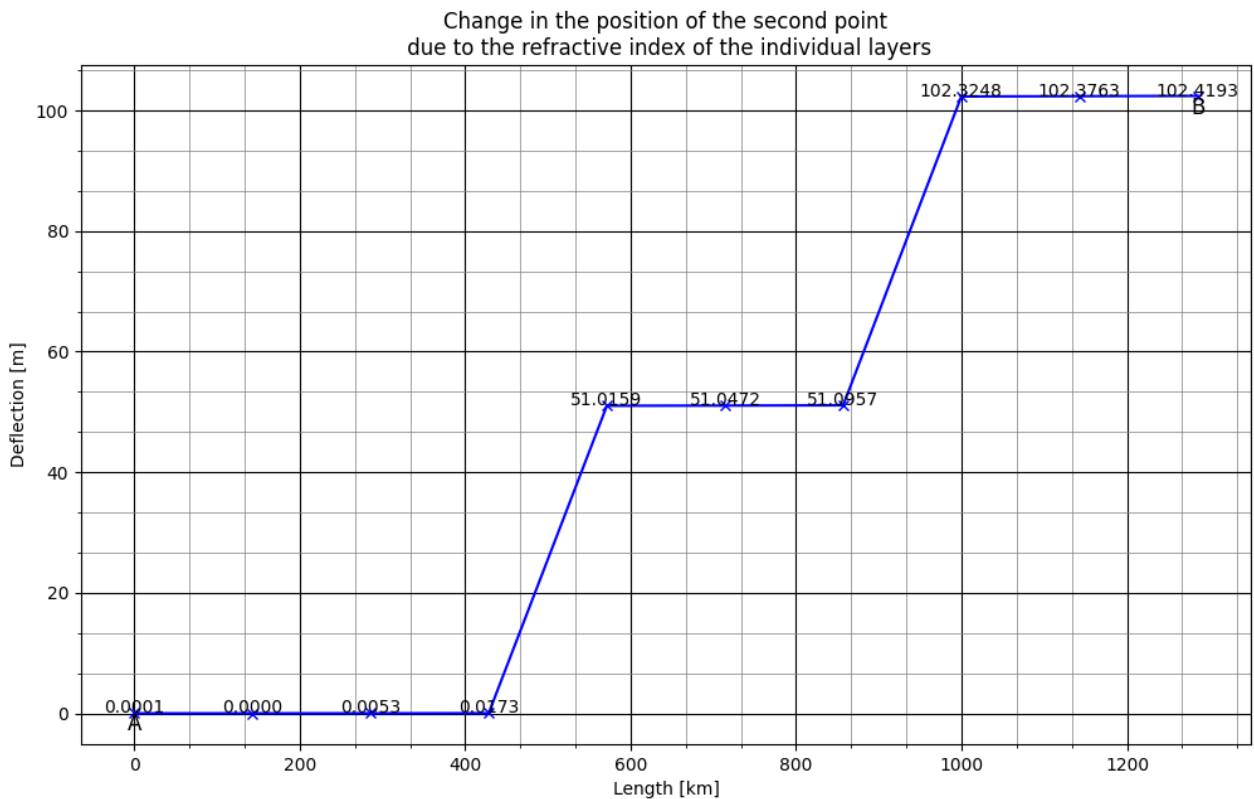


Fig. 3.22 The result of beam propagation between two points separated by land

### 3.2.4 Program limitations

As surface temperatures change for the North and South Poles, with most of the North Pole frozen in the winter months and the sea at the South Pole freezing in the summer months, these areas are considered land, even though in certain places there is a layer of ice under which the index of refraction could be calculated. This problem could be another of the smaller targets for improving and stabilizing the created program.

Another limitation that can be encountered is the above-mentioned choice of salinity for the calculations of individual refractive indices which is constant. However, a dataset containing salinity values can be found and the program could be modified with it.

It should be mentioned that to calculate the deflection of the second point when calculating changes in the refractive index on the path between two points, it is necessary to choose points with different depths, otherwise only the calculation of the change in the refractive index itself is performed.

Another modification of the program could be the addition of optional refractive indices to the route, showing unwanted and erratic turbulence and currents in the water environment, which need to be considered when designing optical transmitters and receivers.

The accuracy is approximately  $0.5^\circ$ , which is mainly governed by the maximum depth dataset used, which is available with values given in  $0.5^\circ$  latitude and longitude increments.

### 3.2.5 Earth relief map

Based on available bathymetry datasets [10], a world relief map was created for illustration, which can be seen in Figure 3.23. These data are further used in calculations. As can be seen, a major limitation is that this dataset only contains values for sea and ocean depths, but not for inland waters.

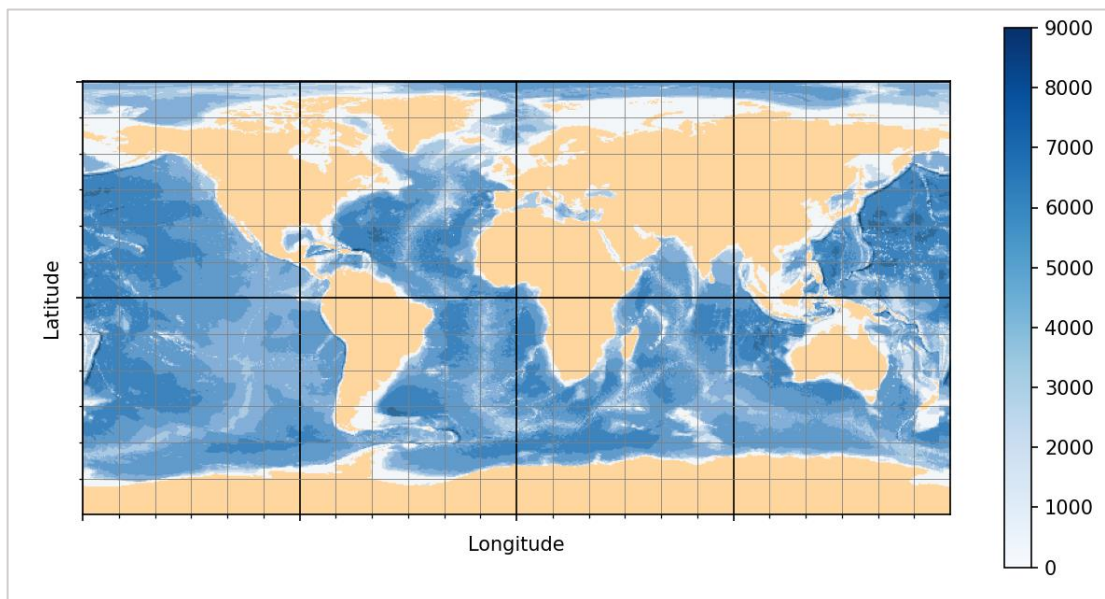


Fig. 3.23 World Relief map

### 3.2.6 Changes in temperature on the path between transmitter and receiver

In the following picture, the demonstration of changes in temperature on the path between two chosen points can be seen.

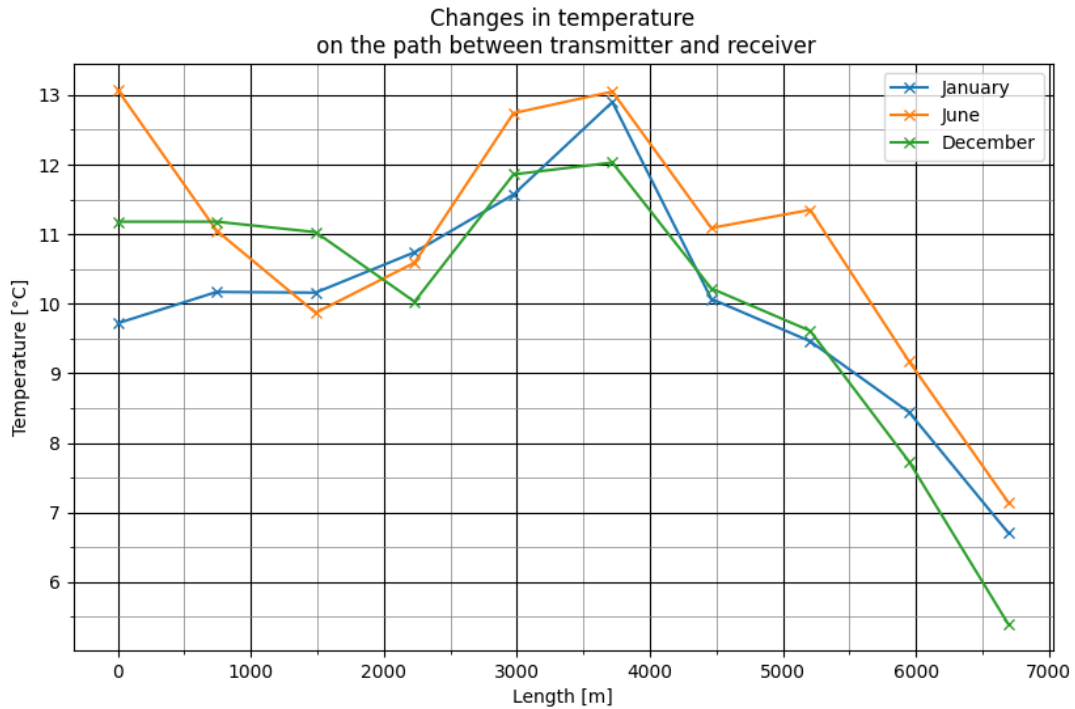


Fig. 3.24 Temperature changes on path between transmitter and receiver

In the graph above, three different temperature changes can be seen for three selected months: January, June, and December. The transmitter was placed at a location with coordinates  $26^{\circ}54'N$  and  $46^{\circ}26'W$ . The receiver's coordinates are  $18^{\circ}28'S$  and  $5^{\circ}40'W$ . The transmitter was placed 500 meters below the surface, and the receiver 1500 meters below the surface. A signal with a wavelength of 400 nm was sent.

In the following Figure 3.25, we can see the connection between the change in the refractive index and the temperature change, the lowest initial temperature for the month of January has the highest initial value of the refractive index, and on the contrary, the highest initial temperature value for the month of June has the lowest initial refractive index. The change in the refractive index on the track in the underwater medium has essentially the inverse course of the temperature change.

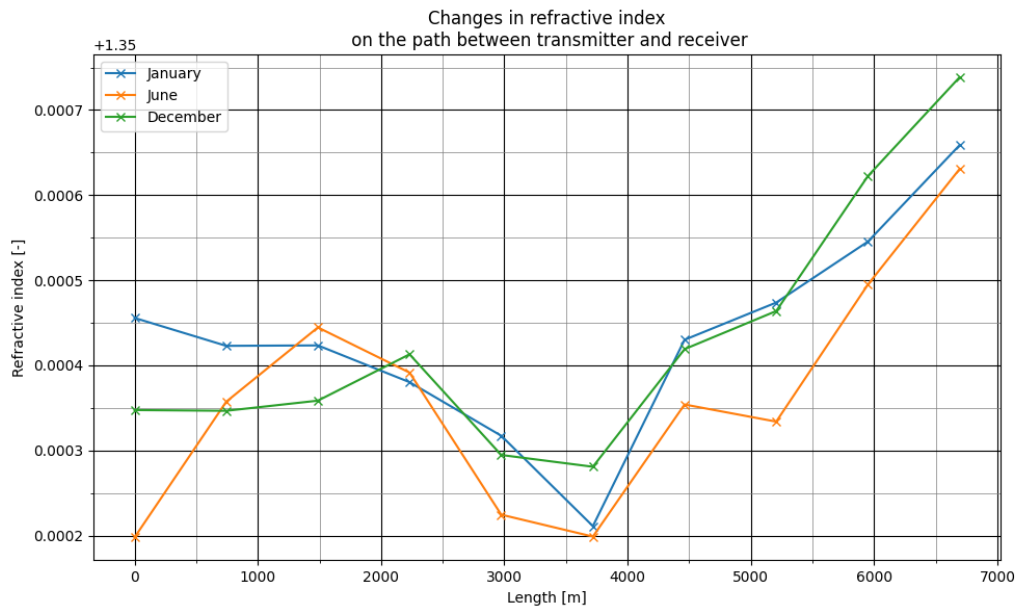


Fig. 3.25 Refractive index changes on path between transmitter and receiver

### 3.2.7 Temperature Profile

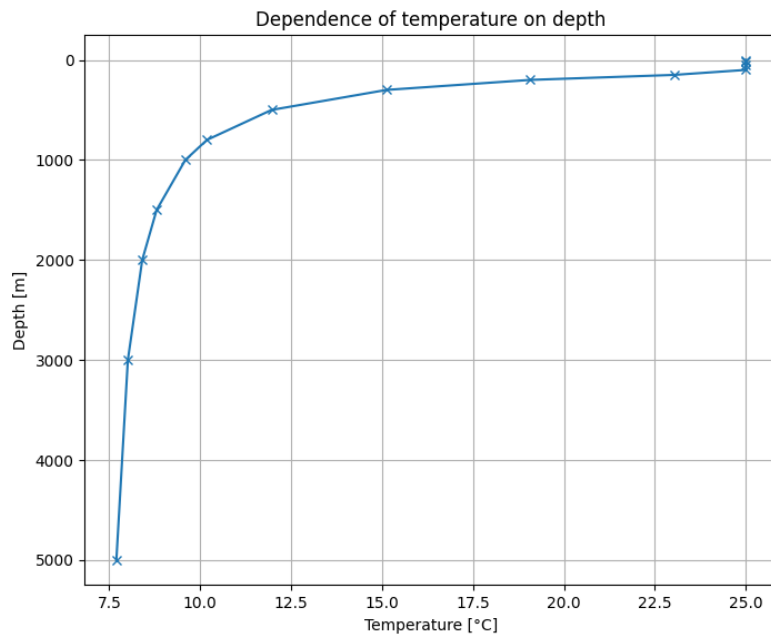
As explained in 1.3.2, temperature decreases rapidly in the so-called thermocline layer. The temperature was calculated using the formula available in [11] and subsequently converted to °C, and in necessary cases, the already mentioned restrictions were applied.

Figure 3.26 shows an example of how the water temperature changes depending on the increasing depth.

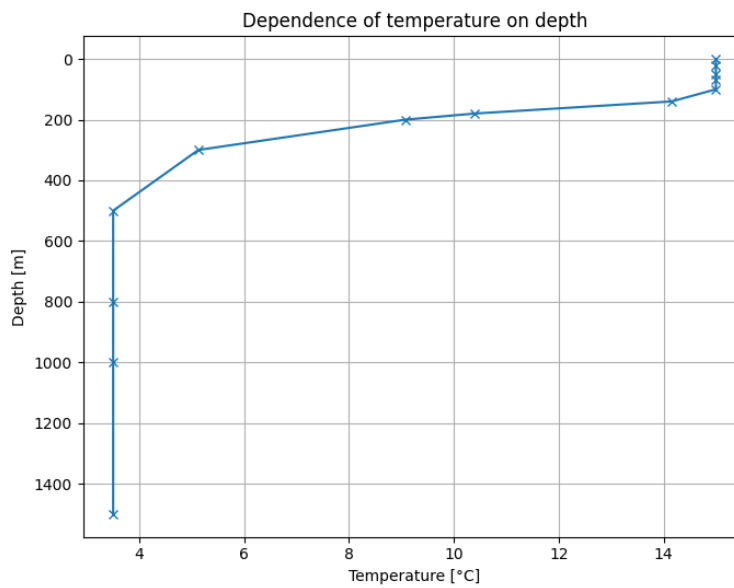
Figure 3.26a) displays the temperature profile for a surface temperature of 25°C. The temperature drops rapidly to a depth of roughly 1000 meters, after which the decrease slows down and the temperature stabilizes around 7.5°C where the maximum depth is over 5000 meters.

Figure 3.26b) shows the temperature profile for a surface temperature of 15°C. The temperature drops rapidly to about 500 meters and is then set as a constant value of 3.5°C to avoid meaningless negative values.

The temperature of the water in the environment is affected by various influences and therefore these calculations are sometimes approximate. Anyway, if the appropriate coordinates and other input parameters are chosen, they are quite accurate. The measurement error then increases with increasing depth and latitude near the poles.



a)



b)

Fig. 3.26 Temperature profile for different surface temperatures

### 3.3 Instructions for Operating the Program

To open the program correctly, it is important to have the main script file *main.py* downloaded, and it is also necessary to have the Excel files of surface temperatures and maximum depths, which are part of the electronic attachment, stored in the same folder. The best way to run the code is to use the PyCharm software, the installation of which is further described in section A.1.

After running the code, first, it is necessary to choose a month from Dropbox to draw the map containing surface temperature values.

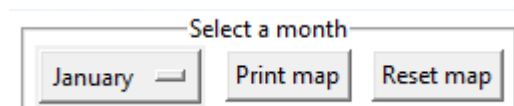


Fig. 3.27 Area for month selection and map rendering

Subsequently, the coordinates of the points are selected. These are entered in the appropriate fields in the form of latitude and longitude with a choice of north or south latitude and east or west longitude. It is necessary to first select the coordinates of the point because then the corresponding surface water temperature and the maximum depth of the given point will be displayed. Only then does the user choose the depth at which the temperature is calculated.

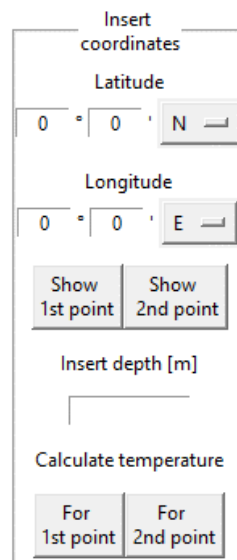
A screenshot of a software interface for entering coordinates and depth. It features several input fields and buttons. At the top, there is a label 'Insert coordinates'. Below it are two rows of input fields: 'Latitude' with '0° 0' N' and 'Longitude' with '0° 0' E'. Below these are two buttons: 'Show 1st point' and 'Show 2nd point'. Below these is a field labeled 'Insert depth [m]'. At the bottom, there is a label 'Calculate temperature' and two buttons: 'For 1st point' and 'For 2nd point'.

Fig. 3.28 Field for entering coordinates and depth below the water surface



If the goal is to detect local changes in the refractive index of the water environment, it is sufficient to enter only the coordinates of the first point. After entering the geographical coordinates and the depth at which the change in the local refractive index will be detected, the type of water environment is selected in the right part of the "Input parameters" section. For seawater, the refractive index is determined with a salinity of 35‰, and for salt water, the salinity is 0‰.

Fig. 3.29 Selecting one point and the choice of type of water environment

Subsequently, it is possible to calculate the local change in the refractive index for the first point. The coordinates of the first point can be changed at any time, just overwrite them, and perform a new temperature calculation at the given depth. When attempting to recalculate the change in the local refractive index, the table of calculated values must first be deleted, then the calculation can be performed again.

Input parameters

Insert coordinates	Select
Latitude 0 ° 0 ' N	Water type <input type="radio"/> Sea water (35‰) <input type="radio"/> Fresh water (0‰)
Longitude 0 ° 0 ' E	Local refractive index changes <input type="button" value="Calculate only index for first point"/> <input type="button" value="Delete table"/>
<input type="button" value="Show 1st point"/> <input type="button" value="Show 2nd point"/>	Changes in index on the path Choose wavelength: <input type="text" value="Wavelength [nm]"/>
Insert depth [m] <input type="text"/>	<input type="button" value="Calculate route between two points"/> <input type="button" value="Do both calculations"/>
Calculate temperature <input type="button" value="For 1st point"/> <input type="button" value="For 2nd point"/>	<input type="button" value="Clear graph 1"/> <input type="button" value="Clear graph 2"/>
Calculated temperature to given depth For the first point is: For the second point is:	

Fig. 3.30 Calculating the local index of refraction and deleting the table

If the goal is to determine the refractive index profile on the path between two points, the coordinates of both points must be entered first. The coordinates are entered in the same fields but displayed with different buttons. For both points, it is necessary to choose the depths in a similar way down below. Subsequently, the type of water environment is chosen. Before the actual calculation, it is important to choose a wavelength from the menu. The wavelength is selected from the range of 400 nm - 700 nm and more significant values for the calculations can be selected. After that, it is possible to proceed to the calculation of the refractive index profile between two points and at the same time to plot the graph of the change in the propagation of the optical beam.

Input parameters

<p><b>Insert coordinates</b></p> <p>Latitude 0 ° 0 ' N</p> <p>Longitude 0 ° 0 ' E</p> <p>Insert depth [m]</p> <p>Calculate temperature</p> <p>For 1st point    For 2nd point</p> <p>Calculated temperature to given depth</p> <p>For the first point is:</p> <p>For the second point is:</p>	<p><b>Select</b></p> <p>Water type</p> <p><input type="radio"/> Sea water (35‰)</p> <p><input type="radio"/> Fresh water (0‰)</p> <p>Local refractive index changes</p> <p>Calculate only index for first point</p> <p>Delete table</p> <p>Changes in index on the path</p> <p>Choose wavelength:</p> <p>Wavelength [nm]</p> <p>Calculate route between two points</p> <p>Do both calculations</p> <p>Clear graph 1    Clear graph 2</p>
--	--

Fig. 3.31 Selecting two different points using different buttons on the left and selecting wavelengths and calculating the refractive index profile on the right

At any time, it is possible to change the map by selecting a different month or returning the map to its original state and deleting all parameters using the "Reset map" button. The button "Do both calculations" enables the calculation of the local change of the refractive index and the profile of the refractive index along the route at the same time. However, it is necessary that all the conditions for these calculations are met, so all the coordinates must be entered, and the type of water environment and the wavelength must be selected.

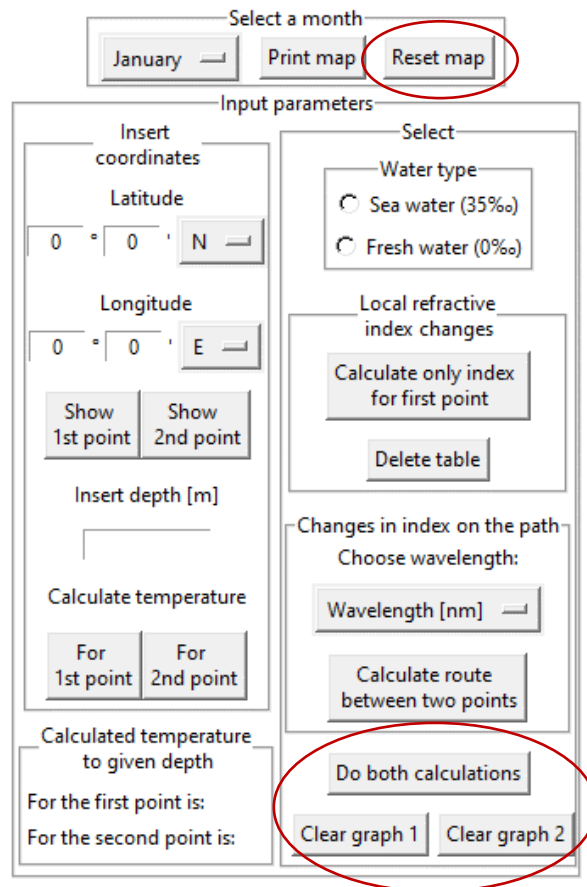


Fig. 3.32 Additional buttons

Figure 3.32 shows the mentioned buttons for resetting the map and for performing both calculations at once. The "Clear graph" buttons are used to delete the content of the drawn graphs of the given calculations. The "Clear graph 1" button clears the contents of the graph of the local refractive index calculation for the first point and "Clear graph 2" removes the area of the graph of changes of the refractive index on the way between two points.

Figure 3.33 is an example of what the program looks like after all calculations have been performed. In the left part, marked in red, are all the selected input parameters, below this part there is a table of calculated index values depending on the wavelength for the first point. The black-marked area on the map shows the points selected by the user. The first point is represented by a black cross, and the second point by a brown one. Below the map there are two graphs, Graph 1 is the plotted dependence of table values for the local change in the refractive index and Graph 2 is the dependence of the change in the refractive index on the route between two points. Next, the deviation graph of the points on this route opens in the external window, which can be seen in Figure 3.33 below the main window.

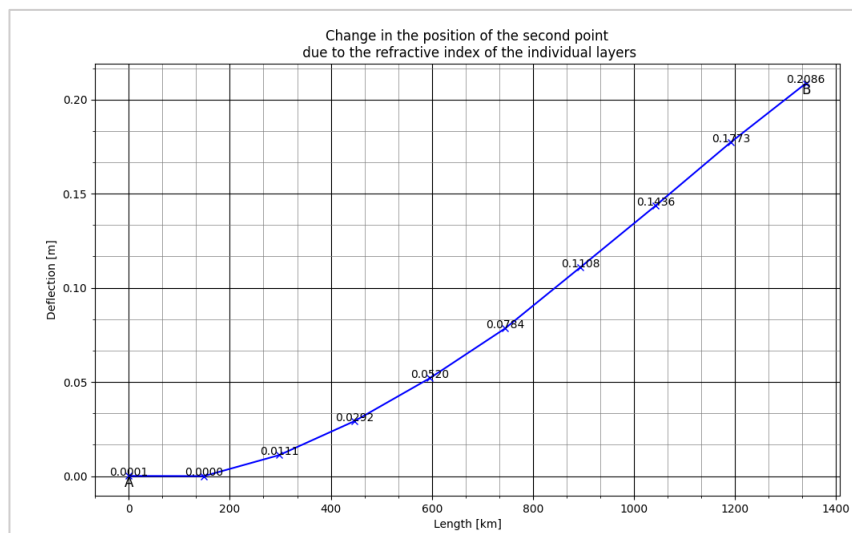
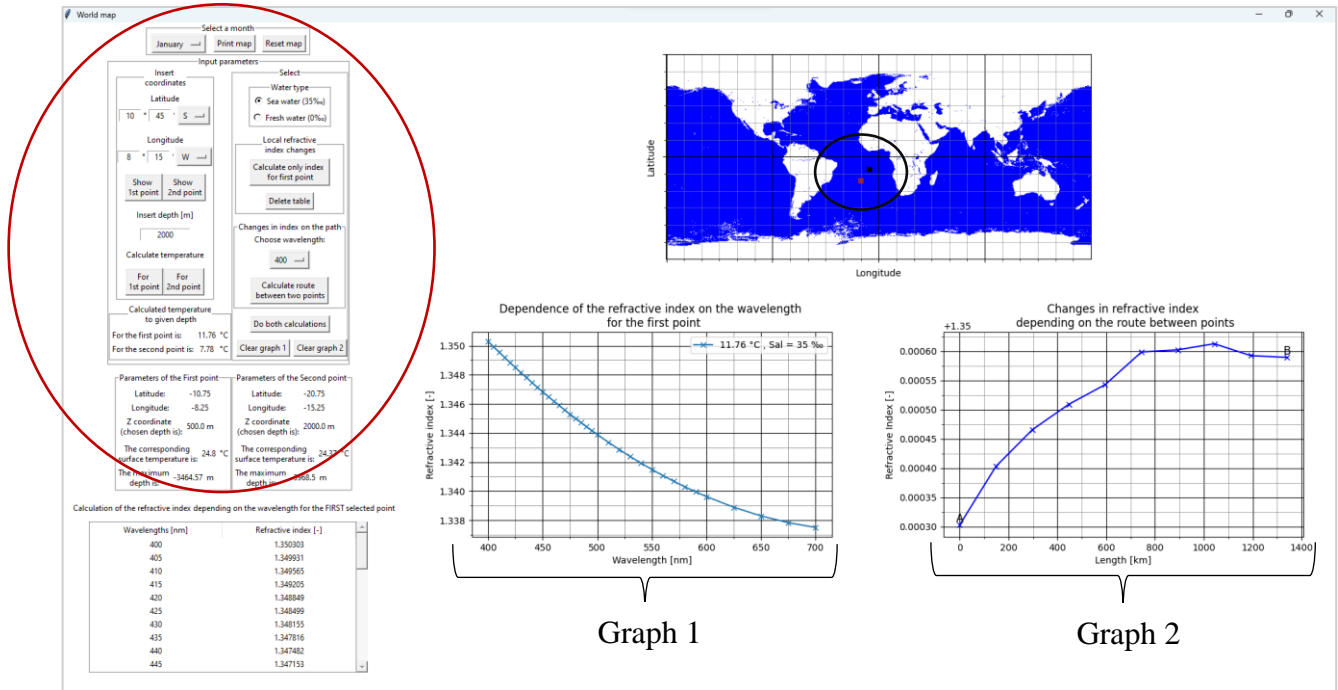


Fig. 3.33 The window of the entire program with the calculation of the deviation on the path between two points

## 4. CONCLUSION

This thesis aimed to create a program that will allow the creation of a world map based on the available datasets and, with the necessary input parameters, determine the refractive index of the water environment for different depths.

In the beginning, the basics of Underwater Communications were presented, the properties and configurations of wireless links used in these communication systems, and the basic properties of the water medium were further analyzed.

In the next stage, the properties of the refractive index and its effect on the UOWC were described, as it changes depending on the wavelength, temperature, depth, etc. Then its expression was carried out using the wave equation from the general Maxwell equations.

The program itself was created using the Python programming language. This language is very intuitive and user-friendly [12], [13]. The function of the program is simple, and a graphical user interface is created when the main program is started. Based on the available datasets of the surface temperatures of the water environment, world maps have been created that vary by each month. These maps also contain datasets of the maximum depths available.

The results of the refractive index calculations are shown in the table and are dependent on both the wavelength and the temperature, which changes depending on the selected depth. These results are plotted as a graph of the dependence of the refractive index on wavelength. In these graphs, the refractive index decreases depending on the increasing wavelength, increases depending on the decreasing temperature, and if the salinity of the water decreases, the refractive index also decreases.

Furthermore, the determination of the refractive index profile of the water environment between two points was achieved based on the selected geographical coordinates and the depth below the water surface. For the route between these points, it was plotted how the propagation of an optical beam of a suitably chosen wavelength changes through this environment. This propagation is also dependent on the selected depth, with which the temperature at a given point is closely related, according to which the refractive index of the underwater environment further changes.

It was also verified that the systems that work in the underwater environment are non-reciprocal, which results in a different course of propagation of the optical beam for two opposite directions of propagation between two points.

## LITERATURE

- [1] KAUSHAL, Hemani a Georges KADDOUM. Underwater Optical Wireless Communication. *IEEE Access*. 2016, 4, 1518-1547. ISSN 2169-3536. doi:10.1109/ACCESS.2016.2552538
- [2] ZENG, Zhaoquan, Shu FU, Huihui ZHANG, Yuhan DONG a Julian CHENG. A Survey of Underwater Optical Wireless Communications. *IEEE Communications Surveys & Tutorials*, vol. 19, no. 1. 2017, 19(1), 204-238. ISSN 1553-877X. doi:10.1109/COMST.2016.2618841
- [3] NOAA. How far does light travel in the ocean?. *National Ocean Service: National Oceanic and Atmospheric Administration* [online]. 11/05/21 [cit. 2022-12-22]. Available from: [https://oceanservice.noaa.gov/facts/light\\_travel.html](https://oceanservice.noaa.gov/facts/light_travel.html)
- [4] NOAA. What is a thermocline? *National Ocean Service: National Oceanic and Atmospheric Administration* [online]. 07/15/21 [cit. 2022-12-25]. Available from: <https://oceanservice.noaa.gov/facts/thermocline.html>
- [5] Refractive Index. *GeegsforGeeks* [online]. Noida, 2021 [cit. 2023-01-01]. Available from: <https://www.geeksforgeeks.org/refractive-index/>
- [6] KULHÁNEK, Petr. *Fyzika II*. Praha: AGA (Aldebaran Group for Astrophysics), 2021.
- [7] Austin, R. W., & Halikas, G. (1976). The index of refraction of seawater. *UC San Diego: Scripps Institution of Oceanography*. Retrieved from <https://escholarship.org/uc/item/8px2019m>
- [8] Index of Refraction of Seawater and Freshwater as a Function of Wavelength and Temperature [online]. 2022 Oregon State University [cit. 25.12.2022]. Available from: <http://research.engr.oregonstate.edu/parrish/index-refraction-seawater-and-freshwater-function-wavelength-and-temperature>
- [9] *Sea Surface Temperature* [online]. Montreal Islands: NASA Earth Observations, 2021 [cit. 2023-01-01]. Available from: <https://neo.gsfc.nasa.gov/view.php?datasetId=MYD28M&year=2021>
- [10] *Bathymetry (GEBCO)* [online]. Montreal Islands: NASA Earth Observations, 2002 [cit. 2022-12-14]. Available from: [https://neo.gsfc.nasa.gov/view.php?datasetId=GEBCO\\_BATHY](https://neo.gsfc.nasa.gov/view.php?datasetId=GEBCO_BATHY)
- [11] Water Temperature at Depth Calculator. *Calculator Academy* [online]. Philadelphia: Academy Team, 2022 [cit. 2023-05-28]. Available from: <https://calculator.academy/water-temperature-at-depth-calculator/>
- [12] Python Programming Language. *GeegsforGeeks* [online]. Noida, 2022 [cit. 2023-01-01]. Available from: <https://www.geeksforgeeks.org/python-programming-language/?ref=shm>
- [13] Python Tutorial. *W3Schools* [online]. c1999-2022 [cit. 2023-01-02]. Available from: <https://www.w3schools.com/python/default.asp>

# SYMBOLS AND ABBREVIATIONS

## Abbreviations:

FEEC	Faculty of Electrical Engineering and Communications
BUT	Brno University of Technology
UOWC	Underwater Optical Wireless Communications
LOS	Line-of-Sight
NLOS	Non-Line-of-Sight
FOV	Field of View
LED	Light Emitting Diode
Gbps	Gigabits per second
Mbps	Megabits per second
kbps	Kilobits per second
ELF	Extremely low frequency
LF	Low frequency
MF	Medium frequency
VHF	Very high frequency
UHF	Ultrahigh frequency
DD	Decimal Degrees
DDM	Degrees with Decimal Minutes

## Symbols:

$n$	Refractive index	(-)
$c_0$	Radiation speed in vacuum	(m/s)
$c$	Radiation speed in a certain medium	(m/s)
$\lambda$	Lambda	(m)
$\nu$	Nu	(Hz)
$\mathbf{B}$	Magnetic induction	(N/Am)
$\mathbf{D}$	Electrical induction	(C/m <sup>2</sup> )
$\mathbf{E}$	Electric field strength	(V/m)
$\mathbf{H}$	Magnetic field strength	(A/m)
$t$	Time	(s)
$\mu$	Permeability	(H/m)
$\varepsilon$	Permittivity	(F/m)
$\rho_Q$	Volume charge density	(C/m <sup>3</sup> )
$\mathbf{j}_Q$	Free current density	(A/m <sup>2</sup> )
$S$	Salinity	(‰)
$T$	Temperature	(°C)
$a, b, c, d, e$	Coefficients for counting refractive index	



# LIST OF APPENDICES

APPENDIX A - PROGRAM IN PYTHON .....	57
APPENDIX B - DATA SETS.....	60

# Appendix A - Program in Python

## A.1 Main source code

Appendix A is a program that was submitted electronically to the system, as its main source code is quite extensive.

It is important to download all the necessary files, the main source code and the datasets of surface temperatures and depths. As the program was created with the language Python in the PyCharm platform, the easiest way to run the code is to download the PyCharm itself. After downloading the PyCharm community package from the JetBrains.com webpage, open the main.py file in the PyCharm program. After opening the file in PyCharm, it is important to choose the Open in program, not the Light version. Subsequently, Python 3.9 is selected as the interpreter in the bar, at the bottom right. The last step before starting will be installing the necessary packages such as "openpyxl", "matplotlib" and "pandas". From now on, the main script should be ready to run.

## A.2 World relief map

```
import tkinter as tk
# import python interface for creating GUI

import numpy as np
# import numpy package for various operations

import pandas as pd
# import pandas package for extracting .xls files

from matplotlib import pyplot as plt
# import pyplot for plotting the map

from matplotlib.backends.backend_tkagg import FigureCanvasTkAgg
# canvas for plotting figures, which can be implemented into Tkinter
as a regular widget

from matplotlib.ticker import (AutoMinorLocator, MultipleLocator)
# used in map figure for grid

# Plotting of world relief map works on similar bases as plotting the
main world map

root = tk.Tk() # main tkinter window

fig = plt.figure(figsize=(10, 5), dpi=150) # create figure for map
plotting
m = fig.add_subplot() # add subplot to the figure
ax = fig.gca() # get axes instance

# import dataset
depths = pd.read_excel('depths.xlsx')
```

```

depths = np.array(depths)

n_rows = len(depths) # 359
n_cols = len(depths[0]) # 720
z = 3
g = np.zeros((n_rows, n_cols, z)) # create 3 matrices of zeros

# set color for each depth
g[depths > 0] = [1., .84, .62]
g[depths <= 0] = [.96, .97, .98]
g[depths <= -1000] = [.82, .88, .94]
g[depths <= -2000] = [.67, .79, .89]
g[depths <= -3000] = [.52, .69, .85]
g[depths <= -4000] = [.38, .61, .8]
g[depths <= -5000] = [.24, .52, .75]
g[depths <= -6000] = [.19, .42, .60]
g[depths <= -7000] = [.14, .31, .46]
g[depths <= -8000] = [.098, .22, .31]
g[depths <= -9000] = [.05, .11, .17]
g[depths <= -10000] = [.01, .4, .7]

shw = ax.imshow(g, cmap='Blues', vmin=0, vmax=9000) # plot the map

# set grid and axes
ax.grid(which='major', color='black', linewidth=0.8)
ax.grid(which='minor', color='grey', linewidth=0.4)

ax.xaxis.set_major_locator(MultipleLocator(n_cols / 4))
ax.set_xlabel("Longitude")
ax.yaxis.set_major_locator(MultipleLocator(n_rows / 2))

ax.xaxis.set_minor_locator(AutoMinorLocator(6))
ax.set_ylabel("Latitude")
ax.yaxis.set_minor_locator(AutoMinorLocator(6))

# create FigureCanvasTkAgg interface between Figure and Map
canvas = FigureCanvasTkAgg(fig, root)
canvas.draw()
canvas.get_tk_widget().pack()

# create colorbar
bar = plt.colorbar(shw)

root.mainloop()

```

## A.3 Changes in temperature on the path between transmitter and receiver

```

from matplotlib import pyplot as plt
# plotting world map with pyplot package

from matplotlib.ticker import (AutoMinorLocator, MultipleLocator)
# used in map figure for grid

import matplotlib as mpl

```

```

x_ax = [0, 743.6843527672786, 1487.3687055345572, 2231.053058301836,
2974.7374110691144, 3718.421763836393,
        4462.106116603672, 5205.79046937095, 5949.474822138229,
6693.159174905508]
temp_jan = [9.72, 10.17, 10.16, 10.74, 11.57, 12.9, 10.07, 9.46, 8.44,
6.71]
temp_june = [13.07, 11.05, 9.87, 10.59, 12.74, 13.05, 11.09, 11.35,
9.17, 7.15]
temp_december = [11.18, 11.18, 11.03, 10.03, 11.86, 12.03, 10.22,
9.61, 7.73, 5.40]
nx_jan = [1.35045571, 1.35042292, 1.35042342, 1.35038023, 1.35031728,
1.35021107, 1.35043004, 1.35047378, 1.35054541, 1.35065868]
nx_june = [1.35019783, 1.35035725, 1.35044455, 1.35039145, 1.35022454,
1.3501988, 1.350354, 1.35033387, 1.35049489, 1.35063071]
nx_decemb = [1.35034747, 1.35034659, 1.35035852, 1.35041296,
1.35029468, 1.35028085, 1.35041905, 1.35046379, 1.35062239,
1.35073851]

# 400 nm
fig = plt.figure(figsize=(8, 6), dpi=100)
ax = fig.gca()
plt.plot(x_ax, nx_jan, marker="x", label='January')

plt.plot(x_ax, nx_june, marker="x", label='June')

plt.plot(x_ax, nx_decemb, marker="x", label='December')

plt.legend()
ax.set_xlabel("Length [m]")
ax.set_ylabel("Refractive index [-]")
ax.set_title("Changes in refractive index\n on the path between
transmitter and receiver")
ax.grid(color='black', linewidth=0.8, which='major')
ax.grid(color='grey', linewidth=0.5, which='minor')
ax.yaxis.set_minor_locator(AutoMinorLocator(2))
ax.xaxis.set_minor_locator(AutoMinorLocator(2))
plt.show()

fig = plt.figure(figsize=(8, 6), dpi=100)
ax = fig.gca()
plt.plot(x_ax, temp_jan, marker="x", label='January')

plt.plot(x_ax, temp_june, marker="x", label='June')

plt.plot(x_ax, temp_december, marker="x", label='December')

plt.legend()
ax.set_xlabel("Length [m]")
ax.set_ylabel("Temperature [°C]")
ax.set_title("Changes in temperature\n on the path between transmitter
and receiver")
ax.grid(color='black', linewidth=0.8, which='major')
ax.grid(color='grey', linewidth=0.5, which='minor')
ax.yaxis.set_minor_locator(AutoMinorLocator(2))
ax.xaxis.set_minor_locator(AutoMinorLocator(2))
plt.show()

```

## **Appendix B - Data sets**

Appendix B contains datasets of surface temperatures and depths in the form of an Excel file, which were again electronically entered into the system. These datasets are an essential part of the source codes.

The *temps.xlsx* file contains the surface temperature datasets and consists of 12 sheets, from January to December.

The *depths.xlsx* file contains is composed of datasets of the maximum depths available.